J. Fluid Mech. (1999), *vol.* 382, *pp.* 109–135. Printed in the United Kingdom

© 1999 Cambridge University Press

The multi-dimensional stability of weak-heat-release detonations

By MARK SHORT AND D. SCOTT STEWART

Theoretical and Applied Mechanics, University of Illinois, Urbana, IL 61801, USA

(Received 27 April 1998 and in revised form 5 October 1998)

The stability of an overdriven planar detonation wave is examined for a one-step Arrhenius reaction model with an order-one post-shock temperature-scaled activation energy θ in the limit of a small post-shock temperature-scaled heat release β. The ratio of specific heats, γ, is taken such that $(\gamma - 1) = O(1)$. Under these assumptions, which cover a wide range of realistic physical situations, the steady detonation structure can be evaluated explicitly, with the reactant mass fraction described by an exponentially decaying function. The analytical representation of the steady structure allows a normal-mode description of the stability behaviour to be obtained via a two-term asymptotic expansion in β. The resulting dispersion relation predicts that for a finite overdrive f, the detonation is always stable to two-dimensional disturbances. For large overdrives, the identification of regimes of stability or instability is found to depend on a choice of distinguished limit between the heat release β and the detonation propagation Mach number D^*. Regimes of instability are found to be characterized by the presence of a single unstable oscillatory mode over a finite range of wavenumbers.

1. Introduction

The hydrodynamic response of a steady planar detonation to two-dimensional linear disturbances in an ideal gas undergoing an irreversible unimolecular reaction with an Arrhenius reaction rate most recently has been investigated numerically by Short & Stewart (1998) using a normal-mode approach. The observed behaviour of the disturbance is found to depend on the structure of the underlying steady detonation wave which is characterized by the size of three parameters: the ratio of specific heats γ and the post-shock temperature-scaled activation energy θ and heat release β. In this formulation, both θ and β depend on the detonation Mach number D^*. Similarly, experimental studies on cellular detonation instabilities show a marked dependence on the chemical sensitivity of the reaction mixture and on the degree of exothermicity of the reaction (Strehlow 1969, 1970; Lee 1984; Kaneshige, Shepherd & Teodorczyk 1997), both of which can be captured by varying the relative sizes of θ and β. Numerical solutions of the nonlinear reactive Euler equations with a one-step Arrhenius reaction model also show that the characteristic cell wavelength and thickness can vary markedly with changes in θ and β (Bourlioux & Majda 1992; Quirk 1994; Williams, Bauwens & Oran 1996; Quirk & Short 1998). One of the major goals of detonation wave research is to understand the hydrodynamic mechanisms underlying the formation of the cellular patterns. Before this can be achieved in general circumstances, a proper understanding of mechanisms controlling the wide range of linear stability responses for varying characteristic detonation parameters must be obtained. Consequently, several asymptotic approaches based on the limiting behaviour of the parameters θ, β and γ previously have been formulated.

https://doi.org/10.1017/S0022112098003759 Published online by Cambridge University Press

Analytical descriptions of the lowest-frequency, two-dimensionally unstable linear modes in the limit of large activation energy θ for both Chapman–Jouguet and overdriven detonations have been provided by Buckmaster & Ludford (1986), Buckmaster (1989), Yao & Stewart (1996), Short (1996), Short & Stewart (1997) and Short (1997*b*). Following Blythe & Crighton (1989), the last three employ the additional assumption of a ratio of specific heats close to unity. Short (1997*b*) has derived a third-order in time and sixth-order in space parabolic linear evolution equation which governs the initial dynamics of cellular detonation formation, and which highlights the important role played by both acoustic wave propagation in the induction zone and curvature of the detonation front.

Recently Clavin, He & Williams (1997) have studied the multi-dimensional stability of overdriven detonation waves in the limit of large propagation Mach numbers D^*. In their article, the appropriateness of using a one-step Arrhenius reaction model to study linear detonation stability in the limit of a large activation energy is questioned. Instead, Clavin *et al.* (1997) use reaction rate models with different temperature sensitivities of the induction zone and main heat release layer to investigate the linear stability problem. As explained in Short (1997*b*), however, their criticisms of the one-step Arrhenius model are based on the error of confusing the *ad hoc* square-wave model due to Zaidel (1961), in which the main reaction layer is assumed *a priori* to have no spatial structure, with that of a detonation model derived using formal asymptotic expansions based on an assumption of large, but finite, activation energy. In this asymptotic context, the large-activation-energy problem is well posed, and comparisons of the behaviour of the lowest-frequency unstable modes, i.e. those in the regimes where the analysis is uniformly valid, with numerically evaluated modes are very favourable (Short & Stewart 1997). In addition, the questions raised by Clavin *et al.* (1997) concerning the limit of an infinite activation energy rather than large but finite activation energies are moot since then, of course, the reference length scale, i.e. the steady half-reaction length, is itself infinite.

Having established the mechanisms behind detonation instability for large activation energies in a one-step Arrhenius reaction model, we now progress to the study of problems with different limits of equally important practical interest, namely those of a moderate activation energy and a low heat release measured on scales associated with the steady post-shock detonation temperature. The latter limit could, for example, account for the large amounts of inert diluent that are typically added to the chemical mixtures when conducting experiments on cellular detonation instabilities (Strehlow 1970), but as in Clavin *et al.* (1997), also covers situations of large detonation overdrive. The former limit could model the presence of a hydrocarbon reactive mixture rather than a hydrogen-oxygen mixture (Fickett, Jacobson & Schott 1972). In the present analysis, we again return to a one-step Arrhenius reaction rate model, and investigate the stability problem in the limits $\theta = O(1)$, $(\gamma - 1) = O(1)$ and $\beta \ll 1$. Here β and θ are scaled such that $\beta = \gamma\widetilde{Q}/\tilde{c}_s^{*2}$ and $\theta = \gamma\widetilde{E}/\tilde{c}_s^{*2}$, where $\widetilde{Q}$ and $\widetilde{E}$ are the actual dimensional heat release and activation energy respectively for the reaction mixture and $\tilde{c}_s^{*2}$ is the immediate post-shock temperature in the steady detonation wave. Since $\tilde{c}_s^{*2}$ is a function of the Mach number D^*, the quantities β and θ represent what will be called respectively the effective heat release and the effective activation energy. Our analysis thus applies to situations where $\widetilde{Q} \ll \tilde{c}_s^{*2}$ and $\widetilde{E} = O(\tilde{c}_s^{*2})$. It is also assumed that the steady post-shock flow Mach number M_s^* is of order unity and that the detonation overdrive $f > 1$, to eliminate the complex transonic flow problem that occurs when $f = 1$, $\beta \ll 1$ and $M_s^* = 1 + O(\beta^{1/2})$. Since

https://doi.org/10.1017/S0022112098003759 Published online by Cambridge University Press

$M_s^* = O(1)$ and $(\gamma - 1) = O(1)$, the analysis here applies to a much wider range of parameters than those considered by Clavin *et al.* (1997), where $\gamma \sim 1$ and $M_s^* \ll 1$.

The advantage of the limits investigated in the present analysis for a one-step Arrhenius reaction model is that the steady detonation structure can be described analytically, with the reactant mass fraction following a simple exponential decay law. By using a two-term perturbation expansion in β, an explicit analytical representation of the normal-mode linear disturbances is obtained, giving rise to an analytical dispersion relation governing the stability of detonations for situations where $\theta = O(1)$ and $\beta \ll 1$. In contrast, the dispersion relation in Clavin *et al.* (1997) is an integral relation and must be obtained by numerical integrations of the perturbation eigenstructures through the spatially varying main reaction zone. Similarly, such integrations would need to be conducted for an analytical investigation of the rationally derived three-step chain-branching reaction model used in Short & Dold (1996) and Short & Quirk (1997) to study the linear stability of a detonation having different temperature sensitivities of the chain-initiation, chain-branching and chain-termination rates. In the present analysis, the growth rate is determined explicitly as a function of the ratio of specific heats γ, the effective heat release β, the effective activation energy θ, the detonation Mach number D^* and the disturbance wavenumber k. This allows us to establish distinguished limits between β and D^* which determine, for example, regimes of stability or instability. In turn, some of the suggestions put forward by Erpenbeck (1964) regarding the existence of such regimes can now be qualified mathematically as a result of the present investigation.

2. Model

An ideal gas $\mathscr{F}$ is assumed to undergo a unimolecular, first-order, irreversible reaction

$$\mathscr{F} \rightarrow \mathscr{P},$$

for product $\mathscr{P}$, with constant mole fraction and ratio of specific heats γ. The reaction rate is modelled by the one-step Arrhenius reaction

$$\frac{\mathrm{D}Y}{\mathrm{D}t} = r = K(1 - Y)\exp\left[-\theta/\left(p/\rho\right)\right], \tag{2.1}$$

where Y is the reaction progress variable, θ is the activation energy for the reaction, K the constant pre-exponential factor and p and ρ are the pressure and density respectively. Unburnt fuel corresponds to $Y = 0$, fully depleted fuel to $Y = 1$. The convective derivative is

$$\frac{\mathrm{D}}{\mathrm{D}t} = \frac{\partial}{\partial t^l} + u_1^l \frac{\partial}{\partial x^l} + u_2^l \frac{\partial}{\partial y^l},$$

where the superscript l on Cartesian space coordinates (x, y), on velocity components (u_1, u_2) and on the time coordinate t denotes the laboratory frame. The caloric and ideal thermal equations of state are respectively

$$e = \frac{p}{(\gamma - 1)\rho} - q, \quad T = p/\rho, \tag{2.2}$$

for specific internal energy e, temperature T and chemical energy q, where

$$q = \beta Y, \tag{2.3}$$

with β representing the total chemical energy available in the unreacted mixture. The model is completed by assuming the hydrodynamic behaviour of the fluid obeys

https://doi.org/10.1017/S0022112098003759 Published online by Cambridge University Press

the compressible reactive Euler equations in which heat-conduction, viscosity and radiation effects are negligible. In non-dimensional form these are

$$\frac{\mathrm{D}\rho}{\mathrm{D}t} + \rho\nabla\cdot\boldsymbol{u} = 0, \quad \frac{\mathrm{D}\boldsymbol{u}}{\mathrm{D}t} + \frac{v}{\gamma}\nabla p = 0, \quad \frac{\mathrm{D}e}{\mathrm{D}t} + p\frac{\mathrm{D}v}{\mathrm{D}t} = 0, \tag{2.4}$$

with the velocity vector denoted by $\boldsymbol{u} = (u_1, u_2)$ and the specific volume by $v = \rho^{-1}$.

The scales for density, pressure, temperature and velocity are the dimensional post-shock density, pressure, temperature and sound speed ($\tilde{c}_s^*$) respectively in an appropriately defined steady detonation wave (see §3). The scaling for length is the steady half-reaction length ($\tilde{l}_{1/2}$), the distance from the shock to the point where half of the reactant is consumed, and for time is $\tilde{l}_{1/2}/\tilde{c}_s^*$. The scaled activation energy and heat release quantities θ and β are defined as

$$\theta = \gamma\widetilde{E}/\tilde{c}_s^{*\,2}, \quad \beta = \gamma\widetilde{Q}/\tilde{c}_s^{*\,2}, \tag{2.5}$$

for dimensional activation energy $\widetilde{E}$ and heat release $\widetilde{Q}$. The alternative scalings are the activation energy E and heat release Q defined by Erpenbeck (1964) as

$$E = \gamma\widetilde{E}/\tilde{c}_0^{*\,2}, \quad Q = \gamma\widetilde{Q}/\tilde{c}_0^{*\,2}, \tag{2.6}$$

where $\tilde{c}_0^*$ is the adiabatic pre-shock sound speed. Defined in this way, E and Q are independent of the detonation speed. Thus,

$$\theta = E/v^2, \quad \beta = Q/v^2, \tag{2.7}$$

where

$$v^2 = \frac{\tilde{c}_s^{*\,2}}{\tilde{c}_o^{*\,2}} = \frac{(2\gamma D^{*\,2} - \gamma + 1)\left[(\gamma - 1) + 2/D^{*\,2}\right]}{(\gamma + 1)^2} \tag{2.8}$$

is the temperature jump across the steady detonation shock. The quantity D^* denotes the detonation Mach number relative to the upstream unreacted material.

3. Steady detonation structure

The standard reactive flow model described in §2 admits a steady one-dimensional steady-wave solution, denoted in the following by the superscript $*$, whose general spatial structure for arbitrary values of γ, θ and β can be determined through a Rankine-Hugoniot analysis with the one-step Arrhenius rate law. Assuming the steady detonation to propagate to the left along the path $x^l = -D_s^* t^l$, where D_s^* is the steady detonation Mach number relative to the post-shock sound speed, the pressure, velocity and density satisfy the relations

$$p^* = a + (1-a)\left[1 - (\gamma-1)\beta b Y^*\right]^{1/2}, \quad u_1^* = \frac{(1-p^*)}{\gamma M_s^*} + M_s^*, \quad u_2^* = 0, \quad \rho^* = \frac{M_s^*}{u_1^*}, \tag{3.1}$$

in the steady shock-attached coordinate system

$$X = x^l + D_s^* t^l, \tag{3.2}$$

where

$$M_s^{*\,2} = \frac{(\gamma-1)D^{*\,2} + 2}{2\gamma D^{*\,2} - (\gamma - 1)}, \quad a = \frac{\gamma M_s^{*2} + 1}{(\gamma + 1)}, \quad b = \frac{2(\gamma+1)M_s^{*2}}{\gamma(1 - M_s^{*\,2})^2}. \tag{3.3}$$

https://doi.org/10.1017/S0022112098003759 Published online by Cambridge University Press

The quantity M_s^* is the flow Mach number immediately behind the shock. The variation in the reaction progress variable is determined by the first-order equation

$$Y_X^* = r^*/u_1^*, \tag{3.4}$$

which defines the constant pre-exponential factor K as

$$K = \int_0^{1/2} u_1^*(1-Y^*)^{-1} \exp\left[\theta/\left(p^*/\rho^*\right)\right] \mathrm{d}Y^*. \tag{3.5}$$

The steady variables satisfy the shock conditions

$$\rho^* = p^* = T^* = 1, \quad u_1^* = M_s^*, \quad u_2^* = 0, \quad Y^* = 0. \tag{3.6}$$

For given γ and β, the detonation velocity D^* is determined by specification of the detonation overdrive, f, defined by

$$f = \left(D^*/D_{CJ}^*\right)^2, \tag{3.7}$$

where D_{CJ}^* is the Chapman–Jouguet (CJ) detonation velocity, the minimum sustainable steady velocity determined by the flow velocity being exactly sonic at the end of the wave where $q^* = \beta$. The corresponding value of M_s^* when $D^* = D_{CJ}^*$ is

$$M_s^* = \left[\left(1+\frac{(\gamma^2-1)\beta}{\gamma}\right) - \left(\left(1+\frac{(\gamma^2-1)\beta}{\gamma}\right)^2 - 1\right)^{1/2}\right]^{1/2}, \tag{3.8}$$

where

$$D_{CJ}^* = \left[\left(1+\frac{(\gamma^2-1)Q}{\gamma}\right) + \left(\left(1+\frac{(\gamma^2-1)Q}{\gamma}\right)^2 - 1\right)^{1/2}\right]^{1/2}. \tag{3.9}$$

Finally, the local flow Mach number M^* is denoted by

$$M^* = u_1^*/\left(p^*/\rho^*\right)^{1/2}, \tag{3.10}$$

where $M^* = 1$ when $q^* = \beta$ corresponds to $D^* = D_{CJ}^*$.

3.1. *The limit of weak effective heat release* $\beta \ll 1$

In the following, practical situations where the post-shock scaled heat release β is small, i.e. $\beta \ll 1$, and the difference between the ratio of specific heats and unity is of order unity, i.e. $(\gamma - 1) = O(1)$, are examined. Since $\beta = Q/v^2$, where v is a function of D^*, we are thus not only concerned with problems where the pre-shock scaled heat release is small, i.e. where $Q \ll 1$, but also with a more general class of problems where $Q \ll v^2$. In order to establish a perturbation procedure, the product of $(\gamma - 1)$ and β is defined as

$$(\gamma-1)\beta = \epsilon, \quad \epsilon \ll 1. \tag{3.11}$$

At this stage an additional restriction is also introduced, in which the flow shock number $M_s^* = O(1) < 1$. Consequently, it is also required that $f > 1$, i.e. the steady wave must be overdriven, in order to eliminate the complex transonic flow problem that occurs when $f = 1$, $\beta = O(\epsilon)$ and $M_s^{*2} = 1 + O(\epsilon^{1/2})$. The assumption $M_s^* = O(1)$ also allows a more general class of problems to be considered than those appearing in Clavin *et al.* (1997), who consider $M_s^* = o(1)$; the present choice ensures that leading-order changes in the flow field propagated along characteristic acoustic wave surfaces can be distinct from those propagated along entropy paths.

https://doi.org/10.1017/S0022112098003759 Published online by Cambridge University Press

Before proceeding, we mention two situations of physical importance contained within these assumptions. First, for large overdrive

$$f \gg 1, \quad D^{*2} \gg 1, \quad v^2 \sim D^{*2}, \quad \beta \sim Q/D^{*2} = O(\epsilon), \tag{3.12}$$

indicating that for $f \gg 1$ the proceeding analysis will be valid for $Q \ll D^{*2}$. This includes cases for which $Q \gg 1$. Note that since $(\gamma - 1) = O(1)$, $M_s^* = O(1)$ when $D^{*2} \gg 1$. Also, when $Q = O(1)$, the ordering

$$D^{*2} = O\left(\epsilon^{-1}\right) \tag{3.13}$$

holds. In contrast, for $O(1)$ overdrives

$$f = O(1) > 1, \quad D^{*2} = O(1), \quad v^2 = O(1), \quad \beta \sim Q = O(\epsilon). \tag{3.14}$$

When $(\gamma - 1) = O(1)$, the last condition thus restricts the validity of the following analysis to situations where $Q = O(\epsilon)$ when $f = O(1)$. However, since $M_s^* = O(1) < 1$ when $D^* = O(1) > 1$ even for $(\gamma - 1) \ll 1$, the assumption that $(\gamma - 1) = O(1)$ can be relaxed and it is only required that $(\gamma - 1)\beta \ll 1$ for the following analysis to be valid for $f = O(1)$. In both cases it will be assumed that the activation energy

$$\theta = O(1). \tag{3.15}$$

For the case of large overdrives (3.12), E can be as large as D^{*2}, thus rendering the analysis valid in the limit of very large activation energies. In the case of $O(1)$ overdrives (3.14), $E = O(1)$.

3.2. *Steady detonation wave structure for $\epsilon \ll 1$*

When $\epsilon \ll 1$ and $\theta = O(1)$, the steady detonation wave structure can be derived asymptotically. Defining $\boldsymbol{z} = [v,\ u_1,\ u_2,\ p,\ Y]^{\mathrm{T}}$ as the matrix of thermodynamic and chemical quantities, the steady structure (3.1) can be expanded in the limit $\epsilon \to 0$ as

$$\boldsymbol{z}^* \sim \boldsymbol{z}_0^* + \epsilon \boldsymbol{z}_1^*, \tag{3.16}$$

where

$$\left.\begin{aligned} \boldsymbol{z}_0^* &= \left[v_b^*,\ u_b^*,\ 0,\ p_b^*,\ Y_0^*\right]^{\mathrm{T}}, \\ \boldsymbol{z}_1^* &= \left[\frac{(Y_0^* - 1)}{\gamma(1 - M_s^{*2})},\ \frac{M_s^*(Y_0^* - 1)}{\gamma(1 - M_s^{*2})},\ 0,\ -\frac{M_s^{*2}(Y_0^* - 1)}{(1 - M_s^{*2})},\ Y_1^*\right]^{\mathrm{T}}, \end{aligned}\right\} \tag{3.17}$$

and

$$\left.\begin{aligned} v_b^* &= 1 + \epsilon \frac{1}{\gamma(1 - M_s^{*2})} + \epsilon^2 \frac{(\gamma + 1)M_s^{*2}}{2\gamma^2(1 - M_s^{*2})^3}, \\ u_b^* &= M_s^* + \epsilon \frac{M_s^*}{\gamma(1 - M_s^{*2})} + \epsilon^2 \frac{(\gamma + 1)M_s^{*3}}{2\gamma^2(1 - M_s^{*2})^3}, \\ p_b^* &= 1 - \epsilon \frac{M_s^{*2}}{(1 - M_s^{*2})} - \epsilon^2 \frac{(\gamma + 1)M_s^{*4}}{2\gamma(1 - M_s^{*2})^3}. \end{aligned}\right\} \tag{3.18}$$

We note that the leading-order state for pressure, velocity, and specific volume is taken to be p_b^*, u_b^* and v_b^*, i.e. the constant burnt state at the equilibrium point $X = \infty$. Although p_b^*, u_b^* and v_b^* have expansions in ϵ, they are legitimately treated as $O(1)$ constant parameters at this stage, and expanded at an appropriate point later in the analysis. As will be demonstrated later, this choice reflects a desire to

https://doi.org/10.1017/S0022112098003759 Published online by Cambridge University Press

capture the correct form of the characteristic surfaces for acoustic wave propagation at the equilibrium state $X = \infty$. It allows us to avoid the secularities that would otherwise occur in the following stability investigation as $X \to \infty$ by approximating the characteristic surfaces for acoustic wave propagation in the region $X > 0$ by those at the shock state $X = 0$.

Using (3.11), the pre-exponential factor K can be expanded as $K \sim K_0 + \epsilon K_1$, where

$$K_0 = \int_0^{1/2} \frac{u_b^* \mathrm{e}^{[\theta/p_b^* v_b^*]}}{(1 - Y_0^*)} \mathrm{d}Y_0^* = u_b^* \mathrm{e}^{[\theta/p_b^* v_b^*]} \ln 2. \tag{3.19}$$

The equation which determines Y_0^* follows from (3.4) and with the shock conditions (3.6) is given by

$$Y_{0,X}^* = \frac{K_0}{u_b^*}(1 - Y_0^*)\mathrm{e}^{-[\theta/p_b^* v_b^*]}, \quad Y_0^*(0) = 0. \tag{3.20}$$

Its solution is

$$Y_0^* = 1 - \left(\tfrac{1}{2}\right)^X. \tag{3.21}$$

Thus the leading-order reactant mass fraction variation Y_0^* decays exponentially for $X > 0$ and is also independent of the activation energy θ. Similarly, the rate r^* is expanded as $r^* \sim r_0^* + \epsilon r_1^*$, where

$$r_0^* = u_b^* \ln(2)(1 - Y_0^*) = u_b^* \ln(2) \left(\tfrac{1}{2}\right)^X. \tag{3.22}$$

4. Linear stability analysis

The stability of a steady detonation wave in the limit of weak effective heat release now can be investigated using a normal-mode approach. The problem for arbitrary values of θ, β, γ and f has been formulated in Bourlioux & Majda (1992), Short (1997*a*), Sharpe (1997) and Short & Stewart (1998). The latter formulation is summarized briefly as follows. The stability analysis proceeds by defining the shock-attached coordinate system

$$x = x^l + D_s^* t^l - h(y, t), \quad t = t^l, \tag{4.1}$$

where $h(y, t)$ represents the perturbation to the shock. Perturbations to the steady detonation wave structure (3.1) and (3.4) have the form

$$\boldsymbol{z} = \boldsymbol{z}^*(x) + \boldsymbol{z}'(x)\mathrm{e}^{\lambda t + \mathrm{i}ky}, \quad h = h'\mathrm{e}^{\lambda t + \mathrm{i}ky}, \tag{4.2}$$

where $\mathrm{Re}(\lambda)$ represents the disturbance growth rate, $\mathrm{Im}(\lambda)$ the disturbance frequency and k the disturbance wavenumber. Substituting (4.1) and (4.2) into (2.1) and (2.4) results in a system of five first-order linear differential equations with spatially varying coefficients for the vector of complex perturbation eigenfunctions $\boldsymbol{z}'(x)$. This system can be written in the form

$$\boldsymbol{A}^* \cdot \boldsymbol{\zeta}_{,x} + \left(\lambda + \mathrm{i}k\boldsymbol{B}^* \cdot + \boldsymbol{C}^* \cdot\right)\boldsymbol{\zeta} - \left(\lambda + \mathrm{i}k\boldsymbol{B}^* \cdot\right)\boldsymbol{z}_x^* = 0, \tag{4.3}$$

where

$$\boldsymbol{\zeta} = \boldsymbol{z}'/h'. \tag{4.4}$$

https://doi.org/10.1017/S0022112098003759 Published online by Cambridge University Press

The matrices $\boldsymbol{A}^*$, $\boldsymbol{B}^*$ and $\boldsymbol{C}^*$ are defined as

$$\boldsymbol{A}^* = \begin{bmatrix} u_1 & -v & 0 & 0 & 0 \\ 0 & u_1 & 0 & v/\gamma & 0 \\ 0 & 0 & u_1 & 0 & 0 \\ 0 & \gamma p & 0 & u_1 & 0 \\ 0 & 0 & 0 & 0 & u_1 \end{bmatrix}^*, \quad \boldsymbol{B}^* = \begin{bmatrix} u_2 & 0 & -v & 0 & 0 \\ 0 & u_2 & 0 & 0 & 0 \\ 0 & 0 & u_2 & v/\gamma & 0 \\ 0 & 0 & \gamma p & u_2 & 0 \\ 0 & 0 & 0 & 0 & u_2 \end{bmatrix}^* \tag{4.5}$$

and

$$\boldsymbol{C}^* = \begin{bmatrix} -u_{1,x} & v_{,x} & 0 & 0 & 0 \\ p_{,x}/\gamma & u_{1,x} & 0 & 0 & 0 \\ 0 & u_{2,x} & 0 & 0 & 0 \\ -(\gamma-1)\beta[r_v - r/v]/v & p_{,x} & 0 & \gamma u_{1,x} - (\gamma-1)\beta r_p/v & -(\gamma-1)\beta r_Y/v \\ -r_v & Y_{,x} & 0 & -r_p & -r_Y \end{bmatrix}^*. \tag{4.6}$$

The undefined quantities in $\boldsymbol{C}^*$ are given by

$$r_v = \frac{r\theta}{vT}, \quad r_p = \frac{r\theta}{pT}, \quad r_Y = -K \exp\left(-\frac{\theta}{T}\right). \tag{4.7}$$

It should be noted that the terms appearing in $\boldsymbol{C}^*$ relating to the first four equations in (4.3) are either proportional to z_x^* or to the factor $(\gamma-1)\beta$. The perturbation shock conditions are determined from the linearized Rankine–Hugoniot shock relations as

$$v' = \lambda\kappa_v h', \quad u_1' = \lambda\kappa_{u_1} h', \quad u_2' = \mathrm{i}k\kappa_{u_2} h', \quad p' = \lambda\kappa_p h', \quad Y' = 0, \tag{4.8}$$

where

$$\kappa_v = \frac{4}{(\gamma+1)D^{*2}M_s^*}, \quad \kappa_{u_1} = \frac{2(1+D^{*2})}{(\gamma+1)D^{*2}}, \quad \kappa_{u_2} = \frac{2M_s^*\left(D^{*2}-1\right)}{2+(\gamma-1)D^{*2}}, \quad \kappa_p = -\frac{4\gamma M_s^*}{(\gamma+1)}. \tag{4.9}$$

The boundary conditions for (4.3) thus become

$$\boldsymbol{\zeta}(0) = \left[\lambda\kappa_v,\ \lambda\kappa_{u_1},\ \mathrm{i}k\kappa_{u_2},\ \lambda\kappa_p,\ 0\right]^{\mathrm{T}}. \tag{4.10}$$

5. Perturbation analysis

A two-term perturbation solution to the differential system (4.3) with boundary conditions (4.10) is now obtained for $\epsilon \ll 1$. Using the steady-state expansion (3.16), the matrices $\boldsymbol{A}^*$, $\boldsymbol{B}^*$ and $\boldsymbol{C}^*$ are each expanded in the regular form

$$\boldsymbol{A}^*(x) = \boldsymbol{A}_0^* + \epsilon\boldsymbol{A}_1^*(x), \quad \boldsymbol{B}^*(x) = \boldsymbol{B}_0^* + \epsilon\boldsymbol{B}_1^*(x), \quad \boldsymbol{C}^*(x) = \boldsymbol{C}_0^*(x) + \epsilon\boldsymbol{C}_1^*(x). \tag{5.1}$$

Similarly, the perturbation eigenfunctions $\boldsymbol{\zeta}$ are also expanded in the regular form

$$\boldsymbol{\zeta} = \boldsymbol{\zeta}_0 + \epsilon\boldsymbol{\zeta}_1. \tag{5.2}$$

https://doi.org/10.1017/S0022112098003759 Published online by Cambridge University Press

5.1. *Leading-order problem*

Substituting equations (5.1) and (5.2) into (4.3) and collecting $O(1)$ terms, the differential system

$$\boldsymbol{A}_0^* \cdot \boldsymbol{\zeta}_{0,x} + \left(\lambda + \mathrm{i}k\boldsymbol{B}_0^* \cdot + \boldsymbol{C}_0^* \cdot\right) \boldsymbol{\zeta}_0 = \left(\lambda + \mathrm{i}k\boldsymbol{B}_0^* \cdot\right) \boldsymbol{z}_{0,x}^* \tag{5.3}$$

is derived which governs the solution for $\boldsymbol{\zeta}_0$. The constant matrices

$$\boldsymbol{A}_0^* = \begin{bmatrix} u_b & -v_b & 0 & 0 & 0 \\ 0 & u_b & 0 & v_b/\gamma & 0 \\ 0 & 0 & u_b & 0 & 0 \\ 0 & \gamma p_b & 0 & u_b & 0 \\ 0 & 0 & 0 & 0 & u_b \end{bmatrix}^*, \quad \boldsymbol{B}_0^* = \begin{bmatrix} 0 & 0 & -v_b & 0 & 0 \\ 0 & 0 & 0 & 0 & 0 \\ 0 & 0 & 0 & v_b/\gamma & 0 \\ 0 & 0 & \gamma p_b & 0 & 0 \\ 0 & 0 & 0 & 0 & 0 \end{bmatrix}^*, \tag{5.4}$$

consist of values of the steady detonation state at the equilibrium point. The matrix $\boldsymbol{C}_0^*$ is given by

$$\boldsymbol{C}_0^* = \begin{bmatrix} 0 & 0 & 0 & 0 & 0 \\ 0 & 0 & 0 & 0 & 0 \\ 0 & 0 & 0 & 0 & 0 \\ 0 & 0 & 0 & 0 & 0 \\ -r_{v0} & Y_{0,x} & 0 & -r_{p0} & -r_{Y0} \end{bmatrix}^*, \tag{5.5}$$

where

$$r_{v0}^* = \frac{r_0^* \theta}{v_b^{*2} p_b^*}, \quad r_{p0}^* = \frac{r_0^* \theta}{v_b^* p_b^{*2}}, \quad r_{Y0}^* = -K_0 \mathrm{e}^{-\left[\theta/p_b^* v_b^*\right]} = -u_b^* \ln 2. \tag{5.6}$$

Thus the equations which determine the leading-order density, pressure and velocity perturbations have constant coefficients and are decoupled from the $O(\epsilon)$ spatial variations in the steady structure brought about by the $O(\epsilon)$ effective heat release and the $O(1)$ spatial gradient variations in Y_0^*. These equations are simply the standard ones of small-amplitude acoustic wave propagation in a uniform medium, with the acoustic perturbations existing around the steady detonation equilibrium state. Writing

$$\boldsymbol{s} = [u_1,\ u_2,\ p]^{\mathrm{T}} \tag{5.7}$$

as the vector of velocity and pressure components, with $\boldsymbol{s} \sim \boldsymbol{s}_0 + \epsilon \boldsymbol{s}_1$, the leading-order solution $\boldsymbol{s}_0$ is simply determined from (5.3) as

$$\boldsymbol{s}_0 = \begin{bmatrix} (u_1)_0 \\ (u_2)_0 \\ p_0 \end{bmatrix} = \begin{bmatrix} A_4 \lambda^{(2)} \\ \mathrm{i}kA_4 \\ \gamma A_1 \end{bmatrix} \mathrm{e}^{\lambda^{(2)} x} + \begin{bmatrix} A_5 \lambda^{(3)} \\ \mathrm{i}kA_5 \\ \gamma A_2 \end{bmatrix} \mathrm{e}^{\lambda^{(3)} x} + \begin{bmatrix} A_6 \\ \mathrm{i}kA_3 \\ 0 \end{bmatrix} \mathrm{e}^{\lambda^{(1)} x}. \tag{5.8}$$

The constants A_1, A_2 and A_3 are undetermined at this stage, while the dependence of A_4, A_5 and A_6 on them is given in Appendix A. The double eigenvalue

$$\lambda^{(1)} = -\frac{\lambda}{u_b^*}, \tag{5.9}$$

https://doi.org/10.1017/S0022112098003759 Published online by Cambridge University Press

corresponds to the propagation of density and vorticity disturbances along entropy waves, while the two eigenvalues

$$\lambda^{(2,3)} = -\frac{u_b^*\lambda}{(u_b^{*\,2} - p_b^* v_b^*)}\left[1 \pm \frac{(p_b^* v_b^*)^{1/2}}{u_b^*}\left[1 + \frac{k^2}{\lambda^2}\left(p_b^* v_b^* - u_b^{*\,2}\right)\right]^{1/2}\right] \tag{5.10}$$

correspond to the characteristic surfaces along which acoustic wave disturbances are propagated. The mode corresponding to $\lambda^{(2)}$ is responsible for acoustic wave disturbances which propagate upstream from the equilibrium point to the detonation shock, while the mode corresponding to $\lambda^{(3)}$ is responsible for acoustic wave disturbances which propagate downstream from the detonation shock to the equilibrium point. Similarly, v_0 is determined as

$$v_0 = \mathrm{A}_8 \mathrm{e}^{\lambda^{(2)}x} + A_9 \mathrm{e}^{\lambda^{(3)}x} + A_7 \mathrm{e}^{\lambda^{(1)}x}, \tag{5.11}$$

where A_7 is yet to be determined, while A_8 and A_9 are given in Appendix A. The last of equations (5.5) determines Y_0 which now depends on the steady, spatially varying reactant mass fraction Y_0^*. This equation can be integrated analytically leading to

$$Y_0 = \ln 2 \left(\tfrac{1}{2}\right)^x \left[(A_{10} + xA_{11})\,\mathrm{e}^{\lambda^{(1)}x} + A_{12}\mathrm{e}^{\lambda^{(2)}x} + A_{13}\mathrm{e}^{\lambda^{(3)}x} + 1\right], \tag{5.12}$$

where A_{10} is yet to be determined, while A_{11}, A_{12} and A_{13} are given in Appendix A.

5.2. *First-order problem*

At the next order of the analysis, the pressure and velocity disturbances are now affected by the spatially varying heat release. The differential system governing $\boldsymbol{\zeta}_1$ can be shown to take the form

$$\begin{aligned}\boldsymbol{A}_0^* \cdot \boldsymbol{\zeta}_{1,x} + \left(\lambda + \mathrm{i}k\boldsymbol{B}_0^* \cdot + \boldsymbol{C}_0^* \cdot\right)\boldsymbol{\zeta}_1 = &-\boldsymbol{A}_1^* \cdot \boldsymbol{\zeta}_{0,x} - \left(\mathrm{i}k\boldsymbol{B}_1^* + \boldsymbol{C}_1^*\right)\cdot \boldsymbol{\zeta}_0 \\ &+ \left(\lambda + \mathrm{i}k\boldsymbol{B}_0^* \cdot\right)\boldsymbol{z}_{1,x}^* + \mathrm{i}k\boldsymbol{B}_1^* \cdot \boldsymbol{z}_{0,x}^*,\end{aligned} \tag{5.13}$$

where the spatially dependent matrices $\boldsymbol{A}_1^*$, $\boldsymbol{B}_1^*$ and $\boldsymbol{C}_1^*$ are defined as

$$\boldsymbol{A}_1^* = \begin{bmatrix} (u_1)_1 & -v_1 & 0 & 0 & 0 \\ 0 & (u_1)_1 & 0 & v_1/\gamma & 0 \\ 0 & 0 & (u_1)_1 & 0 & 0 \\ 0 & \gamma p_1 & 0 & (u_1)_1 & 0 \\ 0 & 0 & 0 & 0 & (u_1)_1 \end{bmatrix}^*, \quad \boldsymbol{B}_1^* = \begin{bmatrix} 0 & 0 & -v_1 & 0 & 0 \\ 0 & 0 & 0 & 0 & 0 \\ 0 & 0 & 0 & v_1/\gamma & 0 \\ 0 & 0 & \gamma p_1 & 0 & 0 \\ 0 & 0 & 0 & 0 & 0 \end{bmatrix}^*, \tag{5.14}$$

https://doi.org/10.1017/S0022112098003759 Published online by Cambridge University Press

and

$$\boldsymbol{C}_1^* = \begin{bmatrix} -(u_1)_{1,x} & v_{1,x} & 0 & 0 & 0 \\ p_{1,x}/\gamma & (u_1)_{1,x} & 0 & 0 & 0 \\ 0 & 0 & 0 & 0 & 0 \\ -\dfrac{r_0}{v_b^{*2}}\left[\dfrac{\theta}{p_b^* v_b^*} - 1\right] & p_{1,x} & 0 & \gamma(u_1)_{1,x} - \dfrac{r_0\theta}{p_b^{*2} v_b^{*2}} & \dfrac{1}{v_b^*} K_0 \mathrm{e}^{-[\theta/p_b^* v_b^*]} \\ -r_{v1} & Y_{1,x} & 0 & -r_{p1} & -r_{Y1} \end{bmatrix}^*. \quad (5.15)$$

Using the $O(\epsilon)$ steady wave structure in §3, the second, third and fourth equations of (5.13) can be written in the form

$$\boldsymbol{F}^* \cdot \boldsymbol{s}_{1,x} + \boldsymbol{G} \cdot \boldsymbol{s}_1 = \left(\tfrac{1}{2}\right)^x \delta \left(\begin{bmatrix} A_{14} \\ \mathrm{i}kA_{17} \\ A_{20} + xA_{21} \end{bmatrix} e^{\lambda^{(1)}x} + \begin{bmatrix} A_{15} \\ \mathrm{i}kA_{18} \\ A_{22} \end{bmatrix} \mathrm{e}^{\lambda^{(2)}x} + \begin{bmatrix} A_{16} \\ \mathrm{i}kA_{19} \\ A_{23} \end{bmatrix} \mathrm{e}^{\lambda^{(3)}x} + \begin{bmatrix} -\lambda^{(1)} u_b^* \ln 2 \\ -\mathrm{i}k v_b^* M_s^* \ln 2 \\ A_{24} \end{bmatrix} \right) \quad (5.16)$$

for $\boldsymbol{s}_1 = [(u_1)_1,\ (u_2)_1,\ p_1]^{\mathrm{T}}$. The coefficients A_{14} to A_{24} are given in Appendix A. Also the matrices $\boldsymbol{F}^*$ and $\boldsymbol{G}^*$ are given by

$$\boldsymbol{F}^* = \begin{bmatrix} 1 & 0 & v_b^*/\gamma u_b^* \\ 0 & 1 & 0 \\ \gamma p_b^*/u_b^* & 0 & 1 \end{bmatrix}, \quad \boldsymbol{G} = \begin{bmatrix} -\lambda^{(1)} & 0 & 0 \\ 0 & -\lambda^{(1)} & \mathrm{i}kv_b^*/\gamma u_b^* \\ 0 & \mathrm{i}k\left[\gamma p_b^*/v_b^*\right] & -\lambda^{(1)} \end{bmatrix} \quad (5.17)$$

and the constant δ by

$$\delta = \frac{M_s^*}{\gamma(1 - M_s^{*2})u_b^*}. \quad (5.18)$$

Since $(1/2)^x$ can be written in the exponential form $\exp[-(\ln 2)x]$ and $\boldsymbol{F}^*$ and $\boldsymbol{G}^*$ are constant, a particular solution for (5.16) can be found as

$$\boldsymbol{s}_{1p} = \left(\tfrac{1}{2}\right)^x \left(\begin{bmatrix} A_{35} + xA_{36} \\ \mathrm{i}k(A_{40} + xA_{41}) \\ A_{30} + xA_{31} \end{bmatrix} \mathrm{e}^{\lambda^{(1)}x} + \begin{bmatrix} A_{37} \\ \mathrm{i}kA_{42} \\ A_{32} \end{bmatrix} \mathrm{e}^{\lambda^{(2)}x} + \begin{bmatrix} A_{38} \\ \mathrm{i}kA_{43} \\ A_{33} \end{bmatrix} \mathrm{e}^{\lambda^{(3)}x} + \begin{bmatrix} A_{39} \\ \mathrm{i}kA_{44} \\ A_{34} \end{bmatrix} \right), \quad (5.19)$$

where the coefficients A_{30} to A_{39} are given in Appendix A. The homogeneous solution to (5.16) has an identical form to (5.8), namely

$$\boldsymbol{s}_{1h} = \begin{bmatrix} (u_1)_{1h} \\ (u_2)_{1h} \\ p_{1h} \end{bmatrix} = \begin{bmatrix} B_4\lambda^{(2)} \\ \mathrm{i}kB_4 \\ \gamma B_1 \end{bmatrix} \mathrm{e}^{\lambda^{(2)}x} + \begin{bmatrix} B_5\lambda^{(3)} \\ \mathrm{i}kB_5 \\ \gamma B_2 \end{bmatrix} \mathrm{e}^{\lambda^{(3)}x} + \begin{bmatrix} B_6 \\ \mathrm{i}kB_3 \\ 0 \end{bmatrix} \mathrm{e}^{\lambda^{(1)}x}, \quad (5.20)$$

https://doi.org/10.1017/S0022112098003759 Published online by Cambridge University Press

where B_1, B_2 and B_3 are undetermined at this stage, and B_4, B_5 and B_6 are given in Appendix A. Thus we have managed to construct a solution for the pressure and velocity normal-mode eigenfunctions $p(x)$, $u_1(x)$, and $u_2(x)$ correct to $O(\epsilon)$, namely

$$\boldsymbol{s} = \boldsymbol{s}_0 + \epsilon(\boldsymbol{s}_{1p} + \boldsymbol{s}_{1h}) + O(\epsilon^2). \tag{5.21}$$

This is now sufficient to determine a dispersion relation for the perturbed weak-effective-heat-release detonation.

6. Radiation condition

In order to determine λ explicitly, an additional condition is required on the perturbations to supplement the shock conditions (4.10). The condition we apply, as originally derived in Buckmaster & Ludford (1986), is that of the standard radiation condition at the equilibrium point $x = \infty$, which prevents acoustic disturbances propagating upstream from $x = \infty$ towards the shock. The characteristic surfaces representing upstream propagation at $x = \infty$ correspond to the modes $\exp\left[\lambda^{(2)}x + \mathrm{i}ky + \lambda t\right]$. Such modes can only be eliminated from the solution (5.8), (5.19) and (5.20) for $\boldsymbol{s}$ by putting

$$A_1 + \epsilon B_1 = 0, \tag{6.1}$$

implying $A_1 = B_1 = 0$. This has the additional implication that the coefficients $A_4 = 0$, $A_8 = 0$, $A_{12} = 0$, $A_{15} = 0$, $A_{18} = 0$, $A_{22} = 0$, $A_{27} = 0$, $A_{32} = 0$, $A_{37} = 0$, $A_{42} = 0$ and $B_4 = 0$ (Appendix A). Thus for the weak-effective-heat-release problem, all upstream acoustic wave propagation is eliminated behind the detonation shock, in contrast to the large-activation-energy problem where upstream acoustic wave propagation is permitted between the main reaction layer and the shock.

7. Shock relations

In order to determine the remaining unknown coefficients A_2, A_3, B_2, B_3, A_7 and A_{10} the shock conditions (4.10) are now employed. The third of equations (5.21) for the pressure perturbation p with (6.1) and (4.10) gives

$$A_2 + \epsilon B_2 = -u_b^* \lambda^{(1)} \gamma^{-1} \kappa_p - \epsilon \gamma^{-1} (A_{30} + A_{33} + A_{34}), \tag{7.1}$$

while the first of equations (5.21) for u_1 with (6.1) and (4.10) gives

$$\frac{k^2}{\lambda^{(1)}} (A_3 + \epsilon B_3) = -\lambda^{(1)} u_b^* \kappa_{u_1} + \frac{v_b^* \lambda^{(3)}}{u_b^* (\lambda^{(3)} - \lambda^{(1)})} (A_2 + \epsilon B_2) - \epsilon (A_{35} + A_{38} + A_{39}), \tag{7.2}$$

$\lambda^{(1)} \neq \lambda^{(3)}$. The second of equations (5.21) for u_2 with (6.1) and (4.10) gives

$$A_3 + \epsilon B_3 = \kappa_{u_2} + \frac{v_b^*}{u_b^* (\lambda^{(3)} - \lambda^{(1)})} (A_2 + \epsilon B_2) - \epsilon (A_{40} + A_{43} + A_{44}). \tag{7.3}$$

Finally, (5.11) and (5.12) with (4.10) give

$$A_7 = \lambda \kappa_v - A_8 - A_9, \quad A_{10} = -A_{12} - A_{13} - 1. \tag{7.4}$$

https://doi.org/10.1017/S0022112098003759 Published online by Cambridge University Press

8. Dispersion relations

8.1. *General dispersion relation*

The dispersion relation governing the stability of detonation waves in the limit of weak effective heat release, $\epsilon \ll 1$, is now obtained by eliminating the combination $A_3 + \epsilon B_3$ from (7.2) and (7.3), with $A_2 + \epsilon B_2$ determined from (7.1). This results in the dispersion relation

$$\lambda^2 \kappa_{u_1} + u_b^* k^2 \kappa_{u_2} - \frac{\gamma^{-1}\kappa_p \lambda^2}{(p_b^*/v_b^*)^{1/2}} \left[1 + \frac{k^2}{\lambda^2}\left(p_b^* v_b^* - u_b^{*2}\right)\right]^{1/2}$$

$$-\epsilon \left[\lambda\left[A_{35} + A_{38} + A_{39}\right] + u_b^* k^2 \left[A_{40} + A_{43} + A_{44}\right]\right.$$

$$\left. - \frac{\gamma^{-1}\lambda}{(p_b^*/v_b^*)^{1/2}}\left[A_{30} + A_{33} + A_{34}\right]\left[1 + \frac{k^2}{\lambda^2}\left(p_b^* v_b^* - u_b^{*2}\right)\right]^{1/2}\right] = 0, \quad (8.1)$$

equivalent to a truncated expansion of the form,

$$F_0(\lambda; a_i(\epsilon)) + \epsilon F_1(\lambda; a_i(\epsilon)) = 0 \quad (8.2)$$

where the constants a_i are $O(1)$.

8.2. *Inert step-shock dispersion relation* ($\epsilon = 0$)

When $Q = 0$ and $(\gamma - 1)$ and D^* are order one, the resulting simplification of (8.1) corresponds to the dispersion relation for inert Euler-step-shock stability. From (8.1) this is, without asymptotic approximation,

$$\lambda^2 \kappa_{u_1} + M_s^* \kappa_{u_2} k^2 - \lambda^2 \gamma^{-1} \kappa_p \left[1 - \frac{k^2}{\lambda^2}(M_s^{*2} - 1)\right]^{1/2} = 0. \quad (8.3)$$

Using (3.3) and (4.9), (8.3) can be written in the form,

$$z^2 + \omega + \xi z^2 \left[1 + \frac{\eta}{z^2}\right]^{1/2} = 0, \quad (8.4)$$

where

$$z = \lambda/k \quad (8.5)$$

and

$$\left.\begin{aligned} \omega = \frac{(\gamma+1)D^{*2}(D^{*2}-1)}{(D^{*2}+1)(2\gamma D^{*2} - (\gamma-1))}, \quad \xi = \frac{2D^{*2}}{(1+D^{*2})}\left(\frac{(\gamma-1)D^{*2}+2}{2\gamma D^{*2}-(\gamma-1)}\right)^{1/2}, \\ \eta = \frac{(\gamma+1)(D^{*2}-1)}{2\gamma D^{*2} - (\gamma-1)}. \end{aligned}\right\} \quad (8.6)$$

Since $1 < \gamma < 2$ and $D^* > 1$, then $\omega > 0$, $\xi > 0$, $\eta > 0$, and it is easily demonstrated that there is no solution of (8.3) with $\mathrm{Re}(\lambda) > 0$. At this point we recall the results of Majda & Rosales (1983) and Majda (1987), who showed that the stability of a step shock in a non-reactive Euler flow for an arbitrary equation of state with a Gruneisen coefficient Γ is governed by the inequality

$$(\mu - 1)M_s^{*2} < (\Gamma + 1)^{-1}, \quad (8.7)$$

where μ represents the ratio of density behind the unperturbed steady planar shock to that downstream of the shock. When the inequality (8.7) is satisfied, the shock is

https://doi.org/10.1017/S0022112098003759 Published online by Cambridge University Press

stable ($\mathrm{Re}(\lambda) < 0$). However, when

$$(\Gamma + 1)^{-1} \leqslant (\mu - 1)M_s^{*2} \leqslant (1 + M_s^*)\Gamma^{-1}, \tag{8.8}$$

the inert step shock is found to be neutrally stable. For

$$(\mu - 1)M_s^{*2} > (1 + M_s^*)\Gamma^{-1} \tag{8.9}$$

the inert step shock is unstable (Erpenbeck 1962). For an ideal gas, $\Gamma = \gamma - 1$, and the inequality (8.7) is satisfied for any finite values of $\gamma > 1$ and $D^* > 1$. When $D^* \to \infty$, however, $(\mu - 1)M_s^{*2} \sim \gamma^{-1}$ and in this limit, as pointed out by Erpenbeck (1962, 1964), the inert Euler step shock becomes neutrally stable. Majda & Rosales (1983) use the regime of neutral stability governed by (8.8) to study the formation of transverse shock waves behind a detonation wave which has no spatial structure. Clavin *et al.* (1997) also note that the highly overdriven limit of the detonation model they examine would be, to leading-order, an inert strong shock. However, explicit analytical solutions for the associated stability problem would still not be possible even in this limit, as is the case for the present detonation model.

8.3. *Stability results for* $D^* = O(1)$, $(\gamma - 1)Q \ll 1$

As well as applying to an inert step shock, the dispersion relation (8.3) also must govern the leading-order stability behaviour of a planar one-step Arrhenius reaction for $D^* = O(1)$ and $\epsilon \ll 1$, i.e. for finite detonation Mach numbers. Based on the discussion in §8.1, the following conclusion can be drawn: when $D^* > D_{CJ}^*$ is finite, $v^2 = O(1)$, $\beta \sim O(Q)$, and the planar detonation is stable ($\mathrm{Re}(\lambda) < 0$) for parameters contained within the limits

$$f = O(1) > 1, \quad (\gamma - 1)Q \ll 1, \quad \theta^{-1} \gg (\gamma - 1)Q. \tag{8.10}$$

The last condition follows from the fact that the leading-order dispersion relation (8.3) for $D^* = O(1) > 1$ is valid for activation energies θ such that $\theta\epsilon \ll 1$. The relations in (8.10) include two cases of particular interest: first, when $(\gamma - 1) = O(1)$ and $Q \ll 1$; and secondly, when $(\gamma - 1) \ll 1$ and $Q = O(1)$. Thus for $(\gamma - 1) = O(1)$ and $f = O(1) > 1$, a detonation with a pre-shock temperature-scaled heat release $Q \ll 1$ will be stable. However, even when $Q = O(1)$, the detonation will remain stable provided $(\gamma - 1) \ll 1$, i.e. in the Newtonian limit, where the ratio of specific heats is sufficiently close to unity. Since $E \sim O(\theta)$ when $f = O(1) > 1$, the relation (8.10) defines a region in the (Q, E, γ, f)-space where the detonation will be stable to two-dimensional disturbances.

8.4. *Dispersion relation for* $D^* \gg 1$ *and* $\epsilon \ll 1$

We now turn our attention to situations where $D^* \gg 1$, so that the inert step shock is, in the limit, neutrally stable (Erpenbeck 1964; Majda & Rosales 1983; Majda 1987). In order to maintain our assertion that $M_s^* = O(1) < 1$, the condition $(\gamma - 1) = O(1)$ is also enforced. For $D^* \gg 1$ the steady-flow Mach number M_s^* has the expansion

$$M_s^* \sim (M_s^*)_0 + \frac{1}{D^{*2}}(M_s^*)_1 + \frac{1}{D^{*4}}(M_s^*)_2, \tag{8.11}$$

where

$$(M_s^*)_0 = \left(\frac{(\gamma - 1)}{2\gamma}\right)^{1/2}, \ (M_s^*)_1 = \frac{(\gamma + 1)^2}{4\gamma\,(2\gamma(\gamma - 1))^{1/2}}, \ (M_s^*)_2 = \frac{(3\gamma - 1)(\gamma - 3)(\gamma + 1)^2}{32\gamma^2(\gamma - 1)\,(2\gamma(\gamma - 1))^{1/2}}. \tag{8.12}$$

https://doi.org/10.1017/S0022112098003759 Published online by Cambridge University Press

Also when $D^{*2} \gg 1$, the constants κ_v, κ_{u_1}, κ_{u_2} and κ_p (4.9) can be expanded in the form

$$\mathscr{F} \sim (\mathscr{F})_0 + \frac{1}{D^2}(\mathscr{F})_1, \tag{8.13}$$

where

$$(\kappa_v)_0 = 0, \quad (\kappa_{u_1})_0 = \frac{2}{\gamma+1}, \quad (\kappa_{u_2})_0 = \left(\frac{2}{\gamma(\gamma-1)}\right)^{1/2}, \quad (\kappa_p)_0 = -\frac{2(2\gamma(\gamma-1))^{1/2}}{\gamma+1}, \tag{8.14}$$

and

$$\left.\begin{aligned} (\kappa_v)_1 &= \frac{4(2\gamma)^{1/2}}{(\gamma+1)(\gamma-1)^{1/2}}, \quad (\kappa_{u_1})_1 = \frac{2}{\gamma+1}, \\ (\kappa_{u_2})_1 &= -\frac{(\gamma+1)(3\gamma-1)}{2\sqrt{2}(\gamma-1)^{3/2}\gamma^{3/2}}, \quad (\kappa_p)_1 = -\frac{(\gamma+1)}{(2\gamma(\gamma-1))^{1/2}}. \end{aligned}\right\} \tag{8.15}$$

Since Q and D^* can be chosen independently, the latter depending on the degree of the overdrive f as well as Q, i.e. $D^* = D^*(\gamma, f, Q)$, the steady equilibrium state p_b^*, u_b^* and v_b^* (3.18) can be expanded as

$$\left.\begin{aligned} p_b^* &\sim 1 - \epsilon\frac{(\gamma-1)}{(\gamma+1)} - \epsilon^2\frac{(\gamma-1)^2}{(\gamma+1)^2} - \frac{\epsilon}{D^{*2}}\frac{(\gamma-1)}{2\gamma}, \\ v_b^* &\sim 1 + \epsilon\frac{2}{(\gamma+1)} + \epsilon^2\frac{4(\gamma-1)}{(\gamma+1)^2} + \frac{\epsilon}{D^{*2}}\frac{1}{\gamma}, \\ u_b^* &\sim \left(\frac{(\gamma-1)}{2\gamma}\right)^{1/2} + \epsilon\frac{(2\gamma(\gamma-1))^{1/2}}{\gamma(\gamma+1)} + \frac{1}{D^{*2}}\frac{(\gamma+1)^2}{4\gamma(2\gamma(\gamma-1))^{1/2}} + \epsilon^2\frac{2(\gamma-1)}{(\gamma+1)^2} \\ &\quad \times \left(\frac{(\gamma-1)}{2\gamma}\right)^{1/2} + \frac{1}{D^{*4}}\frac{(3\gamma-1)(\gamma-3)(\gamma+1)^2}{32\gamma^2(\gamma-1)(2\gamma(\gamma-1))^{1/2}} + \frac{\epsilon}{D^{*2}}\frac{(3\gamma-1)}{2\gamma(2\gamma(\gamma-1))^{1/2}}, \end{aligned}\right\} \tag{8.16}$$

for $D^* \gg 1$ and $\epsilon \ll 1$. The form of these expansions indicates that there are two particular cases of interest which involve choosing distinguished limits between ϵ and D^*. The first occurs in the limit of large overdrives f and for an order-one heat release Q, i.e. for

$$f \gg 1, \quad Q = O(1), \quad \text{where} \quad \epsilon \sim Q/v^2 = O\left(\frac{1}{D^{*2}}\right) \tag{8.17}$$

since for $Q = O(1)$, $D_{CJ}^{*2} = O(1)$ and thus $v^2 \sim D^{*2} = O(f)$. The second again occurs for a large detonation overdrive, but now for a large heat release Q, i.e. when

$$f \gg 1, \quad Q \gg 1, \quad \text{and} \quad \epsilon \sim Q/v^2 \gg O\left(\frac{1}{D^{*2}}\right), \tag{8.18}$$

where $D_{CJ}^{*2} = O(Q)$ and $v^2 \sim D^{*2}$. For the latter situation, we mainly restrict our attention to the two sub-cases

$$Q \gg 1, \quad f \sim O(Q), \quad \epsilon = O\left(\frac{1}{D^*}\right), \tag{8.19}$$

where $D_{CJ}^{*2} = O(Q)$, $v = O(D^*)$ and $D^* = O(Q)$, and

$$Q \gg 1, \quad f \ll O(Q), \quad \epsilon \gg \frac{1}{D^*}, \tag{8.20}$$

https://doi.org/10.1017/S0022112098003759 Published online by Cambridge University Press

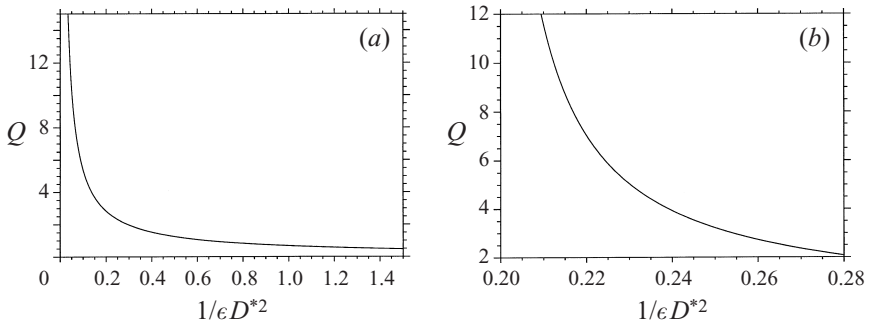


FIGURE 1. (*a*) Q versus $(\epsilon D^{*2})^{-1}$ for $f = 5$ and $\gamma = 1.4$. (*b*) f versus $(\epsilon D^{*2})^{-1}$ for $Q = 2.5$ and $\gamma = 1.4$.

where $D^{*2}_{CJ} = O(Q)$, $v = O(D^*)$ and $D^* = O((fQ)^{1/2})$. The additional case where

$$Q \gg 1, \quad f \gg O(Q), \quad \epsilon \ll \frac{1}{D^*}, \tag{8.21}$$

also having $D^{*2}_{CJ} = O(Q)$, $v = O(D^*)$ and $D^* = O((fQ)^{1/2})$, is covered by the relation (8.18), but requires some additional comments which are given below. Figure 1(*a*) shows the relation between Q and $(\epsilon D^{*2})^{-1}$ for $f = 5$ and $\gamma = 1.4$. Regimes for which $(\epsilon D^{*2})^{-1}$ can be considered as order one are observed to occur where $Q = O(1)$. Figure 1(*b*) shows the relation between f and $(\epsilon D^{*2})^{-1}$ for $Q = 2.5$ and $\gamma = 1.4$.

When any of the distinguished limits (8.17), (8.18), (8.19) or (8.20) hold, p^*_b, u^*_b and v^*_b can be written in the form

$$\mathscr{G} \sim (\mathscr{G})_0 + \epsilon\,(\mathscr{G})_1 + \epsilon^2\,(\mathscr{G})_2\,, \tag{8.22}$$

to $O(\epsilon^2)$, where $(\mathscr{G})_i$ is to be determined from (8.16). At this stage an expansion for the eigenvalue λ is introduced where

$$\lambda \sim \lambda_0 + \epsilon\lambda_1 + \epsilon^2\lambda_2. \tag{8.23}$$

Although at first this appears to be inconsistent with the expansion (8.2), it is shown below that F_0 is not differentiable at $\lambda = \lambda_0$ and $\epsilon = 0$, and (8.2) is sufficient to determine λ to $O(\epsilon^2)$.

Substituting (8.11), (8.13), (8.22) and (8.23) into (8.1) then leads to the following equation for λ_0:

$$\lambda_0^2 + \frac{(\gamma+1)}{2\gamma}k^2 + \left(\frac{2(\gamma-1)}{\gamma}\right)^{1/2}\lambda_0^2\left[1 + \frac{(\gamma+1)}{2\gamma}\frac{k^2}{\lambda_0^2}\right]^{1/2} = 0. \tag{8.24}$$

It is readily observed that the solution

$$\lambda_0 = \pm \mathrm{i}k\left(\frac{(\gamma+1)}{2\gamma}\right)^{1/2} \tag{8.25}$$

occurs when the square root vanishes, and this is precisely when the boundary of transition from stability to neutral stability (8.7) and (8.8) of the inert step shock occurs. Thus, to leading-order, λ is a neutrally stable mode which varies linearly with the wavenumber k. As noted by Clavin *et al.* (1997), a similar result would also hold for their chemical reaction model in the limit of weak effective heat release, but this also must be true for any rationally formulated model reaction scheme such as that investigated by Short & Quirk (1997).

https://doi.org/10.1017/S0022112098003759 Published online by Cambridge University Press

Having established the leading-order behaviour (8.25) in which the square root in (8.24) vanishes, the dispersion relation (8.1) can be simplified to

$$\lambda^2(\kappa_{u_1})_0 + u_b^* k^2(\kappa_{u_2})_0 - \frac{\gamma^{-1}(\kappa_p)_0\lambda^2}{(p_b^*/v_b^*)^{1/2}}\left[1 + \frac{k^2}{\lambda^2}\left(p_b^* v_b^* - u_b^{*2}\right)\right]^{1/2}$$

$$+\frac{1}{D^2}\left[\lambda_0^2(\kappa_{u_1})_1 + (M_s^*)_0 k^2(\kappa_{u_2})_1\right]$$

$$-\epsilon\left[\lambda_0\left[(A_{35})_0 + (A_{38})_0 + (A_{39})_0\right] + (M_s^*)_0 k^2\left[(A_{40})_0 + (A_{43})_0 + (A_{44})_0\right]\right] = 0, \quad (8.26)$$

where $(A_{35})_0$, $(A_{38})_0$, $(A_{39})_0$, $(A_{40})_0$, $(A_{43})_0$ and $(A_{44})_0$ are the leading-order expressions for the coefficients A_{35}, A_{38}, A_{39}, A_{40}, A_{43} and A_{44} obtained when $D^* = \infty$ and $\epsilon = 0$ from their general form given in Appendix A. With the leading-order behaviour (8.25), the next order of terms generated by the dispersion relation (8.26) occurs at $O(\epsilon^{1/2})$, corresponding to a grouping of $O(\epsilon)$ terms within the square root, i.e.

$$F_0 \sim a_0(\lambda - \lambda_0 + a_1\epsilon)^{1/2}. \quad (8.27)$$

Since the $O((\epsilon)^{1/2})$ terms are not balanced by any other terms outside of the square root, λ_1 is determined by the expression

$$2\left[1 - (u_b^*)_0^2\right]\lambda_1 - \lambda_0\left[(p_b^*)_1 + (v_b^*)_1 - 2(u_b^*)_0(u_b^*)_1\right] = 0. \quad (8.28)$$

Using the relations in (8.16), the solution for λ_1 is given by

$$\lambda_1 = \pm ik\left(\frac{\gamma}{2(\gamma+1)}\right)^{1/2}\left[\frac{2-\gamma}{\gamma}\right] \quad (8.29)$$

for $\epsilon \gg 1/D^{*2}$, and

$$\lambda_1 = \pm ik\left(\frac{\gamma}{2(\gamma+1)}\right)^{1/2}\left[\frac{2-\gamma}{\gamma} - \frac{(\gamma+1)^2}{4\gamma^2\epsilon D^2}\right] \quad (8.30)$$

for $\epsilon = O(1/D^{*2})$. Thus the $O(\epsilon)$ correction to λ_0 is again a purely imaginary root which varies linearly with the wavenumber k.

By collecting terms at $O(\epsilon)$ in the dispersion relation (8.26), an expression for the $O(\epsilon^2)$ component λ_2 can be derived in the following form:

$$\lambda_2 = -\frac{\lambda_1^2}{2\lambda_0} - \frac{k^2}{2\lambda_0}\left[(v_b^*)_2 + (p_b^*)_1(v_b^*)_1 + (p_b^*)_2 - 2(M_s^*)_0(u_b^*)_2 - (u_b^*)_1^2\right] + \frac{\gamma^2}{2\lambda_0(\kappa_p)_0^2}$$

$$\times\left[2\lambda_1(\kappa_{u_1})_0 + \frac{k^2}{\lambda_0}(u_b^*)_1(\kappa_{u_2})_0 + \frac{1}{\epsilon D^{*2}}\left[\lambda_0(\kappa_{u1})_1 + (M_s^*)_0\frac{k^2}{\lambda_0}(\kappa_{u_2})_1\right] - \Sigma\right]^2, \quad (8.31)$$

where

$$\Sigma = \left[(A_{35})_0 + (A_{38})_0 + (A_{39})_0 + (M_s^*)_0\frac{k^2}{\lambda_0}\left[(A_{40})_0 + (A_{43})_0 + (A_{44})_0\right]\right]. \quad (8.32)$$

At this stage a real component in λ now appears. For $\epsilon = O(1/D^{*2})$, $\mathrm{Re}(\lambda_2)$ is

https://doi.org/10.1017/S0022112098003759 Published online by Cambridge University Press

given by

$$\mathrm{Re}(\lambda_2) = \frac{\gamma(\gamma+1)\,(\gamma(\gamma+1))^{1/2}}{4\sqrt{2}(\gamma-1)k}\mathrm{Re}(\Sigma) \times \left[\frac{2\sqrt{2}(\gamma-1)k}{(\gamma+1)\,(\gamma(\gamma+1))^{1/2}} - \frac{1}{\epsilon D^{*2}}k\left(\frac{2}{\gamma(\gamma+1)}\right)^{1/2} \pm \mathrm{Im}(\Sigma)\right], \quad (8.33)$$

while for $\epsilon \gg O(1/D^{*2})$ the second term in the square brackets is omitted. Also, solutions for which the principal branch of the square root in (8.26) is selected require

$$\left[\frac{2\sqrt{2}(\gamma-1)k}{(\gamma+1)\,(\gamma(\gamma+1))^{1/2}} - \frac{1}{\epsilon D^{*2}}k\left(\frac{2}{\gamma(\gamma+1)}\right)^{1/2} \pm \mathrm{Im}(\Sigma)\right] > 0. \quad (8.34)$$

Appendix B gives the corresponding forms of $\mathrm{Im}(\lambda_2)$ when $\epsilon = O(1/D^{*2})$, $\epsilon = O(1/D^*)$, and when $\epsilon \gg O(1/D^*)$. When $\epsilon \ll O(1/D^*)$, additional imaginary terms would appear in λ between $O(\epsilon)$ and $O(\epsilon^2)$. However it can be verified that the result for the real component of λ at $O(\epsilon^2)$ nevertheless would be represented by (8.33).

Expressions for $\mathrm{Re}(\Sigma)$ and $\mathrm{Im}(\Sigma)$ are derived from those in Appendix A when $D^* = \infty$ and $\epsilon = 0$, and take the form

$$\mathrm{Re}(\Sigma) = \frac{(2(\gamma-1))^{1/2}\ln(2)}{(\gamma+1)\sqrt{\gamma}} - \frac{(2\gamma(\gamma-1))^{1/2}}{\gamma^3(\gamma+1)^2\ln(2)}\left[(\gamma^2-1)\,[\theta(\gamma-1)+1]\ln^2(2)\right.$$

$$\left.+4\gamma^2(\gamma-2)k^2\right] + \sqrt{2}\ln(2)\left(\frac{(\gamma-1)}{\gamma}\right)^{1/2}\left\{-\frac{16\gamma^2}{(\gamma+1)}\,(2\gamma-3-\theta(\gamma-1))\,k^4\right.$$

$$+4\ln^2(2)(\gamma-1)\,[\theta(\gamma-1)(\gamma-2)-\gamma(\gamma+1)]\,k^2 + (\gamma-1)(\gamma^2-1)$$

$$\left.\times\ln^4(2)\left[\frac{(\gamma-1)}{\gamma^2}\,[\theta(\gamma-1)+1]-1\right]\right\} \Big/ \left[(\gamma^2-1)\ln^2(2)+4\gamma^2k^2\right]^2, \quad (8.35)$$

and

$$\mathrm{Im}(\Sigma) = \pm k\left[\frac{2\sqrt{2}}{(\gamma+1)\,(\gamma(\gamma+1))^{1/2}} + \frac{2}{\gamma^2}\frac{(2\gamma)^{1/2}\,(\gamma-1)^2}{(\gamma+1)\,(\gamma+1)^{1/2}}\,[\theta-2] - \frac{2\,(2\gamma)^{1/2}}{(\gamma+1)^{1/2}}\right.$$

$$\times\left\{16\gamma^2k^4 + 4\ln^2(2)(\gamma-1)\left[\theta(\gamma-1)(\gamma-3)-\gamma^2+5\gamma-3\right]k^2 + (\gamma^2-1)\right.$$

$$\left.\left.\times\frac{(\gamma-1)}{\gamma^2}\ln^4(2)\left[(\gamma-1)^2\theta-\gamma^2+4\gamma-2\right]\right\}\Big/\left[(\gamma^2-1)\ln^2(2)+4\gamma^2k^2\right]^2\right]. \quad (8.36)$$

They are functions of γ, θ and k alone.

8.5. *Large-wavenumber behaviour*

Numerical calculations of the exact linear stability problem (Short & Stewart 1998) for a one-step Arrhenius model show that detonations appear to be stable to sufficiently high-wavenumber disturbances regardless of the value of the parameters E, Q, γ or f. Although our analysis is only valid for $k = O(1)$, we can use the asymptotic

https://doi.org/10.1017/S0022112098003759 Published online by Cambridge University Press

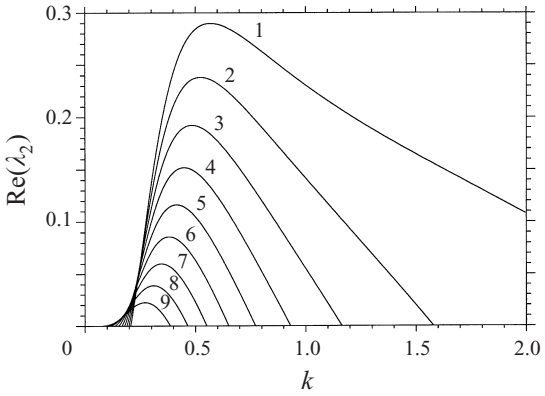


FIGURE 2. Re(λ_2) versus k for $\gamma = 1.4$ and $(\epsilon D^{*2})^{-1} = 0$ with (1) $\theta = 4.5$, (2) $\theta = 4.0$, (3) $\theta = 3.5$, (4) $\theta = 3.0$, (5) $\theta = 2.5$, (6) $\theta = 2.0$, (7) $\theta = 1.5$, (8) $\theta = 1.0$ and (9) $\theta = 0.5$.

expression for the growth rate (8.33) to determine the range of parameters for which the dispersion relation (8.1) predicts stability of the detonation at sufficiently large wavenumbers. From (8.35), as $k \to \infty$

$$\mathrm{Re}(\Sigma) \sim \frac{4\,(2\gamma(\gamma-1))^{1/2}\,(2-\gamma)}{\gamma(\gamma+1)^2\ln(2)}k^2, \tag{8.37}$$

which is positive for $1 < \gamma < 2$. Similarly,

$$\begin{aligned}&\frac{2\sqrt{2}(\gamma-1)k}{(\gamma+1)\,(\gamma(\gamma+1))^{1/2}} - \frac{1}{\epsilon D^{*2}}k\left(\frac{2}{\gamma(\gamma+1)}\right)^{1/2} \pm \mathrm{Im}(\Sigma)\\ &\sim k\left[-\frac{2\,(2\gamma)^{1/2}}{\gamma^2(\gamma+1)\,(\gamma+1)^{1/2}}\left(\gamma^2-3\gamma+3\right) - \frac{1}{\epsilon D^{*2}}\left(\frac{2}{\gamma+1}\right)^{1/2} + \frac{2\,(2\gamma)^{1/2}\,(\gamma-1)^2\theta}{\gamma^2(\gamma+1)\,(\gamma+1)^{1/2}}\right]\end{aligned} \tag{8.38}$$

as $k \to \infty$, so that stability at large wavenumbers occurs provided the inequality

$$(\gamma-1)^2\theta < \gamma^2 - 3\gamma + 3 + \frac{\gamma^2(\gamma+1)\,(\gamma+1)^{1/2}}{2\,(2\gamma)^{1/2}\,\epsilon D^{*2}}\left(\frac{2}{\gamma+1}\right)^{1/2} \tag{8.39}$$

is satisfied. We emphasize, however, that this does not imply instability as $k \to \infty$ for parameters which do not meet this criterion, since (8.33) is not valid in the limit $k \to \infty$. Having obtained an analytical representation of the growth rate (8.33), we proceed to investigate the range of detonation parameters for which stable or unstable solutions can be found.

8.6. *Spectrum for* $\epsilon \gg O(1/D^{*2})$

Figure 2 shows the variation of Re(λ_2) with k calculated from (8.33) for $(\epsilon D^{*2})^{-1} = 0$, $\gamma = 1.4$ and various values of θ. As $k \to 0$,

$$\mathrm{Re}(\lambda_2) \sim -\frac{8\left[\theta(\gamma^2-1) + (-\gamma^2+3\gamma-1)\right]\theta\gamma^2\,(2\gamma)^{1/2}\,(\gamma-1)^{1/2}}{(\gamma+1)(\gamma^2-1)^2\ln^3(2)}k^4, \tag{8.40}$$

so that near $k = 0$, $\partial\mathrm{Re}(\lambda_2)/\partial k < 0$ for $1 < \gamma < 2$. The numerical evaluation of Re(λ_2) from (8.33) reveals that for all values of γ and θ there appears to exist a finite $O(1)$ wavenumber immediately above which Re(λ_2) > 0. Also, providing the inequality

https://doi.org/10.1017/S0022112098003759 Published online by Cambridge University Press

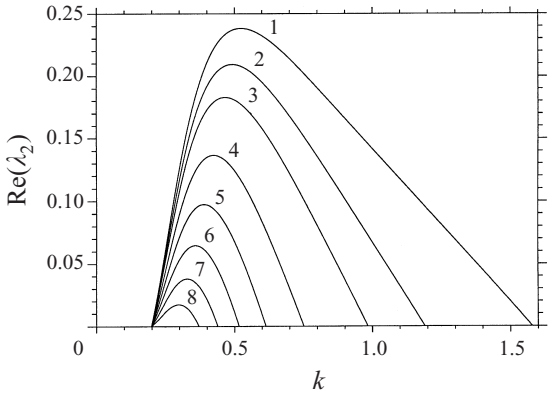


FIGURE 3. The migration of $\mathrm{Re}(\lambda_2)$ with k for $\theta = 4$, $\gamma = 1.4$, and (1) $(\epsilon D^{*2})^{-1} = 0$, (2) $(\epsilon D^{*2})^{-1} = 0.05$, (3) $(\epsilon D^{*2})^{-1} = 0.1$, (4) $(\epsilon D^{*2})^{-1} = 0.2$, (5) $(\epsilon D^{*2})^{-1} = 0.3$, (6) $(\epsilon D^{*2})^{-1} = 0.4$, (7) $(\epsilon D^{*2})^{-1} = 0.5$ and (8) $(\epsilon D^{*2})^{-1} = 0.6$.

(8.39) is satisfied between γ and θ, there is only a finite range of wavenumbers for which $\mathrm{Re}(\lambda_2) > 0$. Both the maximum growth rate and the range of wavenumbers for which $\mathrm{Re}(\lambda_2) > 0$ increase with increasing θ. The wavenumber corresponding to the maximum growth rate found for each θ and γ determines the initial cell size one would expect to observe in the initial stages of the cellular detonation formation process. Thus we conclude that for detonation parameters for which $\epsilon \gg O(1/D^{*2})$, as defined by the distinguished limit (8.18), the detonation is always unstable. Physically, this corresponds to regions of large overdrive $f \gg 1$ and a large pre-shock temperature-scaled heat release $Q \gg 1$.

8.7. *Spectrum for* $\epsilon = O(1/D^{*2})$

Having established that detonations for which $\epsilon \gg O(1/D^{*2})$ are globally unstable, we now establish the stability behaviour in regimes where $\epsilon = O(1/D^{*2})$. Physically, this corresponds to regions of large overdrive $f \gg 1$, but with an order-one heat release Q. Figure 3 shows the behaviour of $\mathrm{Re}(\lambda_2)$ against the wavenumber k calculated from (8.33) with $\theta = 4$, $\gamma = 1.4$ and for various values of $(\epsilon D^{*2})^{-1}$. For each value of $(\epsilon D^{*2})^{-1}$ plotted, there is a finite range of wavenumbers for which $\mathrm{Re}(\lambda_2) > 0$. However, as the parameter $(\epsilon D^{*2})^{-1}$ increases, both the amplitude of the maximum growth rate and the range of unstable wavenumbers decrease. For $(\epsilon D^{*2})^{-1} > 0.7385$, $\theta = 4$ and $\gamma = 1.4$ the detonation becomes stable to two-dimensional disturbances. This general trend was observed for all the values of θ and γ we examined for which there is a finite band of instability for a given value of $(\epsilon D^{*2})^{-1}$, i.e. increasing $(\epsilon D^{*2})^{-1}$ while holding θ and γ fixed will ultimately render the detonation stable.

Figure 4 shows the location of the neutral stability boundaries in the $(\theta, (\epsilon D^{*2})^{-1})$-plane for $\gamma = 1.4$ and $\gamma = 1.6$. The regions to the left of the boundaries are unstable. For $(\epsilon D^{*2})^{-1} \ll 1$, the figure illustrates that no neutral stability boundaries exist. Also, for values of $(\epsilon D^{*2})^{-1}$ and θ for which the detonation is stable, an increase in the activation energy θ for a fixed $(\epsilon D^{*2})^{-1}$, which is equivalent to an increase in E holding γ, Q and f fixed, will eventually render the detonation unstable to two-dimensional disturbances. This feature is in agreement with experimental evidence (Strehlow 1969, 1970) which indicates that detonations in more thermodynamically sensitive reaction mixtures tend to be more unstable. Figure 5 shows the critical value of the wavenumber along the neutral stability boundaries calculated in figure 4. The

https://doi.org/10.1017/S0022112098003759 Published online by Cambridge University Press

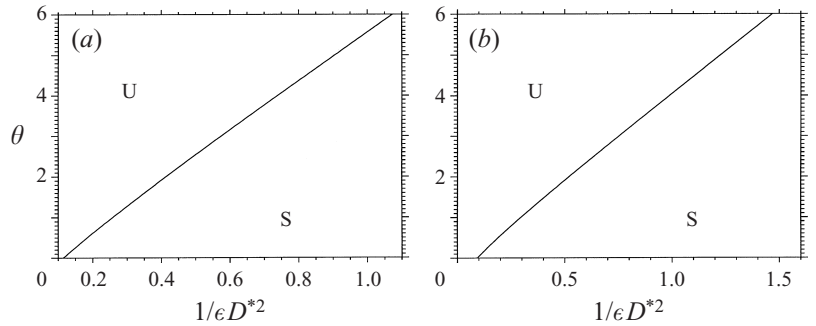


FIGURE 4. The neutral stability boundary in the $(\theta, (\epsilon D^{*2})^{-1})$ plane for (a) $\gamma = 1.4$ and (b) $\gamma = 1.6$. The regions to the left of the neutral stability curve are unstable.

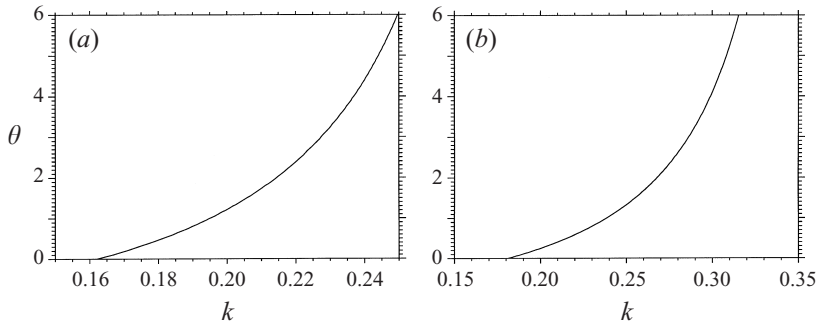


FIGURE 5. The variation of the critical wavenumber along the neutral stability boundaries shown in figure 4 for (a) $\gamma = 1.4$ and (b) $\gamma = 1.6$.

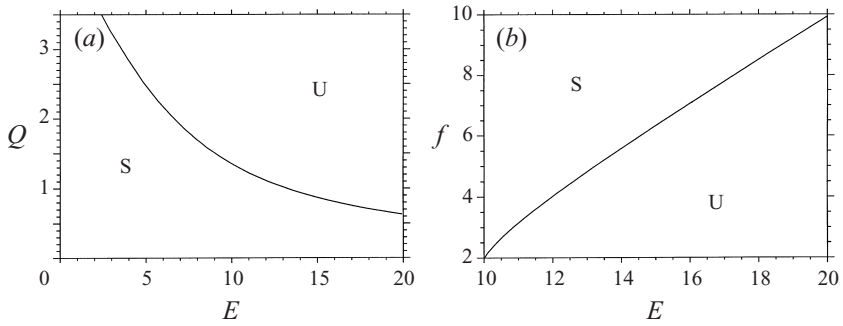


FIGURE 6. The neutral stability boundary in (a) the (Q, E) plane for $\gamma = 1.4$ and $f = 5$, and (b) the (f, E) plane for $\gamma = 1.4$ and $Q = 1$. The regions to the right of the curves are unstable.

neutral stability boundaries shown in figure 4 can also be translated into traditional (Q, E) or (f, E)-planes by using the steady detonation relations in §3. For $f = 5$ and $\gamma = 1.4$, figure 6(a) shows the neutral stability boundary calculated in figure 4(a) in the (Q, E) plane. The region to the right of the boundary is unstable. Our analysis thus predicts that for a fixed activation energy E, overdrive f and ratio of specific heats γ, an increase in Q will drive the detonation into regimes of instability. This boundary is also qualitatively similar to the Q, E neutral stability boundary calculated in Short & Stewart (1998) for lower values of f. Alternatively, figure 6(b) shows the

https://doi.org/10.1017/S0022112098003759 Published online by Cambridge University Press

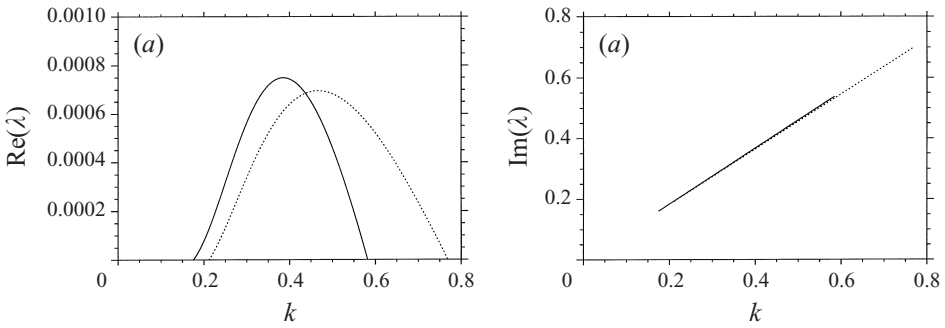


FIGURE 7. Comparison of Re(λ) versus k of the asymptotic solution (solid lines) and a numerical solution (dotted lines) for $Q = 5$, $E = 20$, $f = 5$ and $\gamma = 1.6$. The corresponding values of ϵ, θ and $(\epsilon D^{*2})^{-1}$ are 0.172, 1.146 and 0.10.

neutral stability boundary calculated in figure 4(a) in the (f, E)-plane for $Q = 1$ and $\gamma = 1.4$. Again the region to the right of the boundary is unstable. For a fixed E, an increase in f generally leads to regions where the detonation is stable. Again both these features correspond exactly to the observed experimental behaviour (Strehlow 1969, 1970). The analysis here provides a mechanism for understanding the reasons behind these instabilities in the limit of weak effective heat release. These results also demonstrate that the conjecture by Erpenbeck (1964) that a region of stability should be present for sufficiently high overdrive and low heat release can now be qualified as those regions satisfying the distinguished limit (8.17), i.e. where $Q = O(1)$, and $f \gg 1$. In contrast for $Q \gg 1$ and $f \gg 1$, the detonation is unstable as Erpenbeck (1964) discovered.

Finally, figure 7 shows a typical comparison of the growth rate and frequency obtained from (8.23) with a numerical solution of the full stability problem for $Q = 5$, $E = 20$, $f = 5$ and $\gamma = 1.6$. The three-term approximation of the frequency is clearly excellent. The one-term approximation of the growth rate provides a reasonable approximation of the qualitative features of the growth rate, and could be improved quantitatively by considering higher-order terms in the analysis.

9. Summary

The stability of an overdriven planar detonation wave has been examined for a one-step Arrhenius reaction model in the limit of weak effective heat release $\beta \ll 1$ and an order-one activation energy θ, where β and θ are scaled with respect to the post-shock detonation temperature. These limits allow an analytical dispersion relation to be obtained which governs the stability of a detonation to small-amplitude perturbations. The effective heat release is defined as $\beta = Q/v^2$, where v^2 represents the ratio of the steady post-shock temperature to the pre-shock temperature, and thus depends on the steady detonation propagation Mach number D^*. The parameter Q represents the dimensional heat release scaled with respect to the pre-shock temperature. For $D^* = O(1) > 1$, $Q \ll 1$ and $(\gamma - 1) = O(1)$, or $D^* = O(1) > 1$, $Q = O(1)$ and $(\gamma - 1) \ll 1$, the detonation is globally stable. For overdriven detonations with $D^* \gg 1$ and $(\gamma - 1) = O(1)$, the presence of a neutral boundary can be demonstrated when $Q = O(1)$. Alternatively, for $D^* \gg 1$, $(\gamma - 1) = O(1)$, and $Q \gg 1$, there is a finite band of wavenumbers over which a single unstable oscillatory mode is present.

https://doi.org/10.1017/S0022112098003759 Published online by Cambridge University Press

M.S. was supported by the US Air Force Office of Scientific Research (F49620-96-1-0260). D.S.S. was supported by the US Air Force Wright Laboratories (F08630-94-10004). M.S. is grateful for discussions with Professor P. A. Blythe. The authors are also grateful to Dr J. Yao for assistance with verification of some of the algebra.

Appendix A. Coefficients

The coefficients appearing in (5.8) are given by

$$A_4 = -\frac{v_b^*}{u_b^*}\frac{A_1}{(\lambda^{(2)}-\lambda^{(1)})}, \quad A_5 = -\frac{v_b^*}{u_b^*}\frac{A_2}{(\lambda^{(3)}-\lambda^{(1)})}, \quad A_6 = \frac{k^2 A_3}{\lambda^{(1)}}. \tag{A 1}$$

Similarly the coefficients appearing in (5.11) are determined as

$$A_8 = -\frac{v_b^*}{p_b^*}A_1, \quad A_9 = -\frac{v_b^*}{p_b^*}A_2, \tag{A 2}$$

while those in (5.12) are given by

$$\left.\begin{aligned} A_{11} = \frac{\theta}{v_b^{*2}p_b^*}A_7 - \frac{A_6}{u_b^*}, \quad A_{12} = \frac{1}{(\lambda^{(2)}-\lambda^{(1)})}\left[\frac{\theta(\gamma-1)}{v_b^* p_b^{*2}}A_1 - \frac{A_4\lambda^{(2)}}{u_b^*}\right], \\ A_{13} = \frac{1}{(\lambda^{(3)}-\lambda^{(1)})}\left[\frac{\theta(\gamma-1)}{v_b^* p_b^{*2}}A_2 - \frac{A_5\lambda^{(3)}}{u_b^*}\right]. \end{aligned}\right\} \tag{A 3}$$

The coefficients A_{14} to A_{24} in (5.16) are given by

$$A_{14} = \left[\lambda^{(1)} - \ln(2)\right]A_6 + M_s^* \ln(2) A_7, \tag{A 4}$$

$$A_{15} = A_4\lambda^{(2)}\left[\lambda^{(2)} - \ln(2)\right] + \frac{A_1\lambda^{(2)}}{M_s^*} + M_s^*\ln(2)A_8, \tag{A 5}$$

$$A_{16} = A_5\lambda^{(3)}\left[\lambda^{(3)} - \ln(2)\right] + \frac{A_2\lambda^{(3)}}{M_s^*} + M_s^*\ln(2)A_9, \tag{A 6}$$

$$A_{17} = \lambda^{(1)}A_3, \quad A_{18} = A_4\lambda^{(2)} + \frac{A_1}{M_s^*}, \quad A_{19} = A_5\lambda^{(3)} + \frac{A_2}{M_s^*}, \tag{A 7}$$

$$A_{20} = \gamma M_s^*\ln(2)A_6 + \frac{\ln(2)}{\delta v_b^{*2}}\left[\frac{\theta}{p_b^* v_b^*} - 1\right]A_7 - \frac{1}{v_b^*\delta}\ln^2(2)A_{10}, \quad A_{21} = -\frac{\ln^2(2)}{\delta v_b^*}A_{11}, \tag{A 8}$$

$$\begin{aligned} A_{22} = -\gamma^2 M_s^* A_4\left(\lambda^{(2)}\left[\lambda^{(2)} - \frac{\ln(2)}{\gamma}\right] - k^2\right) \\ + A_1\left(\gamma\lambda^{(2)} + \frac{\ln(2)}{p_b^* v_b^*\delta}\left[\frac{\theta(\gamma-1)}{p_b^* v_b^*} + 1\right] - \gamma^2\ln(2)\right) - \frac{1}{\delta v_b^*}\ln^2(2)A_{12}, \end{aligned} \tag{A 9}$$

https://doi.org/10.1017/S0022112098003759 Published online by Cambridge University Press

$$A_{23} = -\gamma^2 M_s^* A_5 \left(\lambda^{(3)}\left[\lambda^{(3)} - \frac{\ln(2)}{\gamma}\right] - k^2\right)$$

$$+A_2\left(\gamma\lambda^{(3)} + \frac{\ln(2)}{p_b^* v_b^* \delta}\left[\frac{\theta(\gamma-1)}{p_b^* v_b^*} + 1\right] - \gamma^2\ln(2)\right) - \frac{1}{\delta v_b^*}\ln^2(2)A_{13}, \quad \text{(A 10)}$$

$$A_{24} = \gamma M_s^* u_b^* \lambda^{(1)}\ln 2 - \frac{\ln^2(2)}{\delta v_b^*}. \quad \text{(A 11)}$$

The coefficients A_{30} to A_{44} appearing in (5.19) are given by

$$A_{30} = \left[\delta A_{25} - A_{31}\left(2\left[1 - \frac{p_b^* v_b^*}{u_b^{*2}}\right]\left(\lambda^{(1)} - \ln(2)\right) - 2\lambda^{(1)}\right)\right]$$

$$\times\left[\left[1 - \frac{p_b^* v_b^*}{u_b^{*2}}\right]\ln^2(2) + 2\lambda^{(1)}\frac{p_b^* v_b^*}{u_b^{*2}}\ln(2) - \frac{p_b^* v_b^*}{u_b^{*2}}\left(\left[\lambda^{(1)}\right]^2 - k^2\right)\right]^{-1}, \quad \text{(A 12)}$$

$$A_{31} = \delta A_{26}\left[\left[1 - \frac{p_b^* v_b^*}{u_b^{*2}}\right]\ln^2(2) + 2\lambda^{(1)}\frac{p_b^* v_b^*}{u_b^{*2}}\ln(2) - \frac{p_b^* v_b^*}{u_b^{*2}}\left(\left[\lambda^{(1)}\right]^2 - k^2\right)\right]^{-1}, \quad \text{(A 13)}$$

$$A_{32} = \delta A_{27}\left[\left[1 - \frac{p_b^* v_b^*}{u_b^{*2}}\right]\left(-2\lambda^{(2)}\ln(2) + \ln^2(2)\right) + 2\lambda^{(1)}\ln(2)\right]^{-1}, \quad \text{(A 14)}$$

$$A_{33} = \delta A_{28}\left[\left[1 - \frac{p_b^* v_b^*}{u_b^{*2}}\right]\left(-2\lambda^{(3)}\ln(2) + \ln^2(2)\right) + 2\lambda^{(1)}\ln(2)\right]^{-1}, \quad \text{(A 15)}$$

$$A_{34} = \delta A_{29}\left[\left[1 - \frac{p_b^* v_b^*}{u_b^{*2}}\right]\ln^2(2) + 2\lambda^{(1)}\ln(2) + \left[\left[\lambda^{(1)}\right]^2 + \frac{p_b^* v_b^*}{u_b^{*2}}k^2\right]\right]^{-1}, \quad \text{(A 16)}$$

where

$$\left.\begin{aligned}
A_{25} &= -A_{20}\ln(2) + A_{21} - \frac{\gamma p_b^*}{u_b^*}A_{14}\left(\lambda^{(1)} - \ln(2)\right) + \frac{\gamma p_b^*}{u_b^*}k^2 A_{17},\\
A_{26} &= -\ln(2)A_{21},\\
A_{27} &= (\lambda^{(2)} - \lambda^{(1)} - \ln(2))A_{22} - \frac{\gamma p_b^*}{u_b^*}A_{15}\left(\lambda^{(2)} - \ln(2)\right) + \frac{\gamma p_b^*}{u_b^*}k^2 A_{18},\\
A_{28} &= (\lambda^{(3)} - \lambda^{(1)} - \ln(2))A_{23} - \frac{\gamma p_b^*}{u_b^*}A_{16}\left(\lambda^{(3)} - \ln(2)\right) + \frac{\gamma p_b^*}{u_b^*}k^2 A_{19},\\
A_{29} &= -\left(\lambda^{(1)} + \ln(2)\right)A_{24} - M_s^*\frac{\gamma p_b^* v_b^*}{u_b^*}\ln(2)k^2 - \gamma p_b^*\ln^2(2)\lambda^{(1)};
\end{aligned}\right\} \quad \text{(A 17)}$$

$$A_{35} = -\frac{1}{\ln(2)}\left(\delta A_{14} - \frac{v_b^*}{\gamma u_b^*}\left[A_{30}(\lambda^{(1)} - \ln(2)) + \frac{\lambda^{(1)}A_{31}}{\ln(2)}\right]\right), \quad \text{(A 18)}$$

$$A_{36} = \frac{v_b^*}{\gamma u_b^*\ln(2)}\left(\lambda^{(1)} - \ln(2)\right)A_{31}, \quad \text{(A 19)}$$

https://doi.org/10.1017/S0022112098003759 Published online by Cambridge University Press

$$A_{37} = \frac{1}{(\lambda^{(2)} - \lambda^{(1)} - \ln(2))}\left[\delta A_{15} - \frac{v_b^*}{\gamma u_b^*} A_{32}(\lambda^{(2)} - \ln(2))\right], \tag{A 20}$$

$$A_{38} = \frac{1}{(\lambda^{(3)} - \lambda^{(1)} - \ln(2))}\left[\delta A_{16} - \frac{v_b^*}{\gamma u_b^*} A_{33}(\lambda^{(3)} - \ln(2))\right], \tag{A 21}$$

$$A_{39} = \frac{1}{(\lambda^{(1)} + \ln(2))}\left[\delta \lambda^{(1)} u_b^* \ln(2) - \frac{v_b^*}{\gamma u_b^*} \ln(2) A_{34}\right], \tag{A 22}$$

$$A_{40} = -\frac{1}{\ln(2)}\left(\delta A_{17} - \frac{v_b^*}{\gamma u_b^*} A_{30}\right) + \frac{v_b^*}{\gamma u_b^* \ln^2(2)} A_{31}, \tag{A 23}$$

$$A_{41} = \frac{v_b^* A_{31}}{\gamma u_b^* \ln(2)}, \tag{A 24}$$

$$A_{42} = \frac{1}{(\lambda^{(2)} - \lambda^{(1)} - \ln(2))}\left(\delta A_{18} - \frac{v_b^*}{\gamma u_b^*} A_{32}\right), \tag{A 25}$$

$$A_{43} = \frac{1}{(\lambda^{(3)} - \lambda^{(1)} - \ln(2))}\left(\delta A_{19} - \frac{v_b^*}{\gamma u_b^*} A_{33}\right), \tag{A 26}$$

$$A_{44} = \frac{1}{(\lambda^{(1)} + \ln(2))}\left(\delta v_b^* M_s^* \ln(2) + \frac{v_b^*}{\gamma u_b^*} A_{34}\right). \tag{A 27}$$

Finally, the coefficients appearing in (5.20) are given by

$$B_4 = -\frac{v_b^*}{u_b^*}\frac{B_1}{(\lambda^{(2)} - \lambda^{(1)})}, \quad B_5 = -\frac{v_b^*}{u_b^*}\frac{B_2}{(\lambda^{(3)} - \lambda^{(1)})}, \quad B_6 = \frac{k^2 B_3}{\lambda^{(1)}}. \tag{A 28}$$

Appendix B. Calculation of Im(λ_2)

For $\epsilon = O(1/D^{*2})$,

$$\begin{aligned}\mathrm{Im}(\lambda_2) = {} & \mp\frac{\mathrm{i}}{k}\frac{\gamma(\gamma+1)(\gamma(\gamma+1))^{1/2}}{4\sqrt{2}(\gamma-1)} \\ & \times\left[[\mathrm{Re}(\Sigma)]^2 - \left(\frac{2\sqrt{2}(\gamma-1)}{(\gamma+1)(\gamma(\gamma+1))^{1/2}}k - \frac{\sqrt{2}k}{(\gamma(\gamma+1))^{1/2}\epsilon D^{*2}} \pm \mathrm{Im}(\Sigma)\right)^2\right] \\ & \mp\frac{\mathrm{i}k}{2(2\gamma)^{1/2}(\gamma+1)^2(\gamma+1)^{1/2}}\left[(\gamma+1)(2-\gamma)^2 + 2\gamma(\gamma-1)^2\right] \\ & \times\mp\frac{\mathrm{i}k(\gamma+1)^{1/2}(3\gamma-2)}{4\gamma(2\gamma)^{1/2}\epsilon D^{*2}} \mp \frac{\mathrm{i}k(2\gamma)^{1/2}(\gamma+1)^2(5\gamma-3)}{16\gamma^3(\gamma+1)^{1/2}\epsilon^2 D^{*4}}.\end{aligned} \tag{B 1}$$

https://doi.org/10.1017/S0022112098003759 Published online by Cambridge University Press

When $\epsilon = O(1/D^*)$,

$$\mathrm{Im}(\lambda_2) = \mp\frac{\mathrm{i}}{k}\frac{\gamma(\gamma+1)(\gamma(\gamma+1))^{1/2}}{4\sqrt{2}(\gamma-1)}\left[[\mathrm{Re}(\Sigma)]^2 - \left(\frac{2\sqrt{2}(\gamma-1)}{(\gamma+1)\,(\gamma(\gamma+1))^{1/2}}k \pm \mathrm{Im}(\Sigma)\right)^2\right]$$
$$\mp\frac{\mathrm{i}k}{2\sqrt{2\gamma}(\gamma+1)^2\sqrt{\gamma+1}}\left[(\gamma+1)(2-\gamma)^2 + 2\gamma(\gamma-1)^2\right]$$
$$\mp\frac{\mathrm{i}k\,(2\gamma)^{1/2}\,(\gamma+1)\,(\gamma+1)^{1/2}}{8\gamma^2\epsilon^2 D^{*2}}. \tag{B 2}$$

When $\epsilon \gg O(1/D^*)$,

$$\mathrm{Im}(\lambda_2) = \mp\frac{\mathrm{i}}{k}\frac{\gamma(\gamma+1)\sqrt{\gamma(\gamma+1)}}{4\sqrt{2}(\gamma-1)}\left[[\mathrm{Re}(\Sigma)]^2 - \left(\frac{2\sqrt{2}(\gamma-1)}{(\gamma+1)\,(\gamma(\gamma+1))^{1/2}}k \pm \mathrm{Im}(\Sigma)\right)^2\right]$$
$$\mp\frac{\mathrm{i}k}{2\,(2\gamma)^{1/2}\,(\gamma+1)^2\,(\gamma+1)^{1/2}}\left[(\gamma+1)(2-\gamma)^2 + 2\gamma(\gamma-1)^2\right]. \tag{B 3}$$

REFERENCES

Blythe, P. A. & Crighton, D. G. 1989 Shock Generated Ignition: the induction zone. *Proc. R. Soc. Lond.* A **426**, 189–209.

Bourlioux, A. & Majda, A. J. 1992 Theoretical and numerical structure for unstable two-dimensional detonations. *Combust. Flame* **90**, 211–229.

Buckmaster, J. D. 1989 A theory for triple point spacing in overdriven detonation waves. *Combust. Flame* **77**, 219–228.

Buckmaster, J. D. & Ludford, G. S. S. 1986 The effect of structure on the stability of detonations I. Role of the induction zone. In *Twenty-first Symp. (Intl) on Combustion,* pp. 1669–1676. The Combustion Institute.

Clavin, P., He, L. & Williams, F. A. 1997 Multidimensional stability analysis of overdriven gaseous detonations. *Phys. Fluids* **9**, 3764–3785.

Erpenbeck, J. J. 1962 Stability of step shocks. *Phys. Fluids* **4**, 1181–1187.

Erpenbeck, J. J. 1964 Stability of idealized one-reaction detonations. *Phys. Fluids* **7**, 684–696.

Fickett, W., Jacobson, J. D. & Schott, G. L. 1972 Calculated pulsating one-dimensional detonations with induction-zone kinetics. *AIAA J.* **10**, 514–516.

Kaneshige, M., Shepherd, J. E. & Teodorczyk, A. 1997 Detonation database. Graduate Aeronautical Laboratories, California Institute of Technology.

Lee, J. H. S. 1984 Dynamic parameters of gaseous detonations. *Ann. Rev. Fluid Mech.* **16**, 311–336.

Majda, A. J. 1987 Criteria for regular spacing of reacting Mach stems. *Proc. Natl Acad. Sci. USA* **84**, 6011–6014.

Majda, A. J. & Rosales, R. 1983 A theory for spontaneous Mach Stem formation in reacting shock fronts. I: the basic perturbation analysis. *SIAM J. Appl. Maths* **43** 1310–1334.

Quirk, J. J. 1994 Godunov-type schemes applied to detonation flows. In *Combustion in High-Speed Flows* (ed. J. Buckmaster, T. L. Jackson & A. Kumar) pp. 575–596.

Quirk, J. J. & Short, M. 1998 Cellular detonation stability. II: The dynamics of cell formation. In preparation.

Sharpe, G. J. 1997 Linear stability of idealized detonations. *Proc. R. Soc. Lond.* A **453**, 2603–2625.

Short, M. 1996 An asymptotic derivation of the linear stability of the square wave detonation using the Newtonian limit. *Proc. R. Soc. Lond.* A **452**, 2203–2224.

Short, M. 1997*a* Multi-dimensional linear stability of a detonation wave at high-activation energy. *SIAM J. Appl. Maths* **57**, 307–326.

Short, M. 1997*b* A parabolic linear evolution equation for cellular detonation instability. *Combust. Theory Modell.* **1**, 313–346.

https://doi.org/10.1017/S0022112098003759 Published online by Cambridge University Press

Short, M. & Dold, J. W. 1996 Linear stability of a detonation wave with a model three-step chain-branching reaction. *Math. Comput. Modell.* **24**, 115–123.

Short, M. & Quirk, J. J. 1997 On the nonlinear stability and detonability limit of a detonation wave for a model 3-step chain-branching reaction. *J. Fluid Mech.* **339**, 89–119.

Short, M. & Stewart, D. S. 1997 Low-frequency two-dimensional linear instability of plane detonation. *J. Fluid Mech.* **340**, 249–295.

Short, M. & Stewart, D. S. 1998 Cellular detonation stability. I: A normal-mode linear analysis. *J. Fluid Mech.* **368**, 229–262.

Strehlow, R. A. 1969 The nature of transverse wave in detonations. *Astron. Acta* **14**, 539–548.

Strehlow, R. A. 1970 Multi-dimensional detonation wave structure. *Astron. Acta* **15**, 345–357.

Williams, D. N., Bauwens, L. & Oran, E. S. 1996 Detailed structure and propagation of three-dimensional detonations. In *Twenty-sixth Symp. (Intl) on Combustion*, pp. 2991–2998. The Combustion Institute, Pittsburgh.

Yao, J. & Stewart, D. S. 1996 On the dynamics of multi-dimensional detonation waves. *J. Fluid Mech.* **309**, 225–275.

Zaidel, R. M. 1961 The stability of detonation waves in gaseous detonations. *Dokl. Akad. Nauk SSSR (Phys. Chem. Sect.)* **136**, 1142–1145.

https://doi.org/10.1017/S0022112098003759 Published online by Cambridge University Press